Journal of Medicinal Chemistry

pubs.acs.org/jmc Article

Propionamide Derivatives as Dual μ-Opioid Receptor Agonists and σ_1 Receptor Antagonists for the Treatment of Pain

Mónica García,* Virginia Llorente, Lourdes Garriga, Ute Christmann, Sergi Rodríguez-Escrich, Marina Virgili, Begoña Fernández, Magda Bordas, Eva Ayet, Javier Burgueño, Marta Pujol, Albert Dordal, Enrique Portillo-Salido, Georgia Gris, José Miguel Vela, and Carmen Almansa

Cite This: *J. Med. Chem.* 2021, 64, 10139−10154 Read Online

ACCESS | Metrics & More | Article Recommendations | Supporting Information

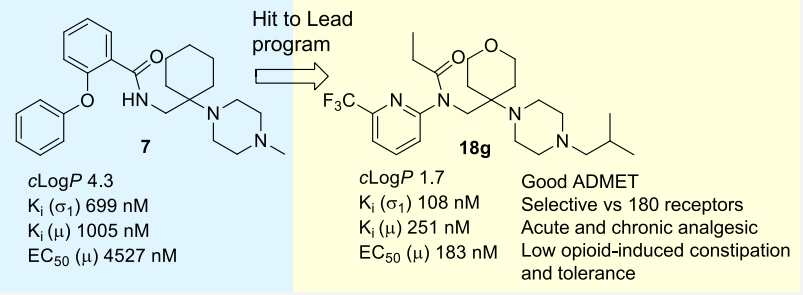

ABSTRACT: A new series of propionamide derivatives was developed as dual μ-opioid receptor agonists and σ_1 receptor antagonists. Modification of a high-throughput screening hit originated a series of piperazinylcycloalkylmethyl propionamides, which were explored to overcome the challenge of achieving balanced dual activity and convenient drug-like properties. The lead compound identified, **18g**, showed good analgesic effects in several animal models of both acute (paw pressure) and chronic (partial sciatic nerve ligation) pain, with reduced gastrointestinal effects in comparison with oxycodone.

INTRODUCTION

Chronic pain is a condition affecting a significant part of the population at some point in their lifetime, and it is associated with significant alterations not only in health but also in quality and life style[1] since it induces affective disorders, such as depression and anxiety, sleep disorders, and different disability levels.[2] As a consequence, chronic pain is one of the great health problems worldwide at present due to both its high prevalence and the economic, social, and psychological costs that it entails.[3] Current therapeutic strategies are only partially effective or carry the risk of severe side effects, as in the case of μ-opioid receptor (MOR) agonists, which are associated with limiting adverse effects such as respiratory depression, nausea, vomiting, and constipation.[4] Moreover, in long-term treatments, opioid drugs induce tolerance,[5,6] and as a consequence, increasing the dosage of opioids is often required throughout the chronic pain treatment to maintain effective pain relief, which finally results in unbearable side effects and/or addiction. Abuse of opioids due to their reinforcement properties[7] has recently led to abuse epidemics affecting the United States with dramatic consequences.[8] Figure 1 shows the structure of three of the most relevant MOR agonists, morphine (**1**), oxycodone (**2**), and fentanyl (**3**).

In view of the multicomponent nature of pain, drugs addressing simultaneous action on multiple targets and showing synergistic efficacy are considered a good way to provide better therapeutic indexes.[9] Further advantages of this approach are (i) potentially reduced side effects due to the possibility of using a relatively lower affinity of multimodal compounds showing a synergistic therapeutic effect, (ii) better treatment compliance in comparison to that of a combination of monomodal drugs, (iii) lower potential for drug−drug interactions, and (iv) a more convenient pharmacokinetic (PK) profile.[10]

With the aim of finding new analgesics with reduced adverse effects, we undertook a research program to discover multimodal compounds with dual σ_1 receptor (σ_1R) antagonistic and MOR agonistic activities. The rationale behind this strategy is linked both to the potentiation of opioid analgesia with σ_1R antagonists[11−14] and to the important effects of σ_1R antagonism in neuropathic pain where opioids are poorly effective.[15,16] The results obtained with σ_1R knockout mice,[17,18] and with several σ_1R antagonists,

Received: March 8, 2021
Published: July 8, 2021

https://doi.org/10.1021/acs.jmedchem.1c00417
J. Med. Chem. 2021, 64, 10139−10154

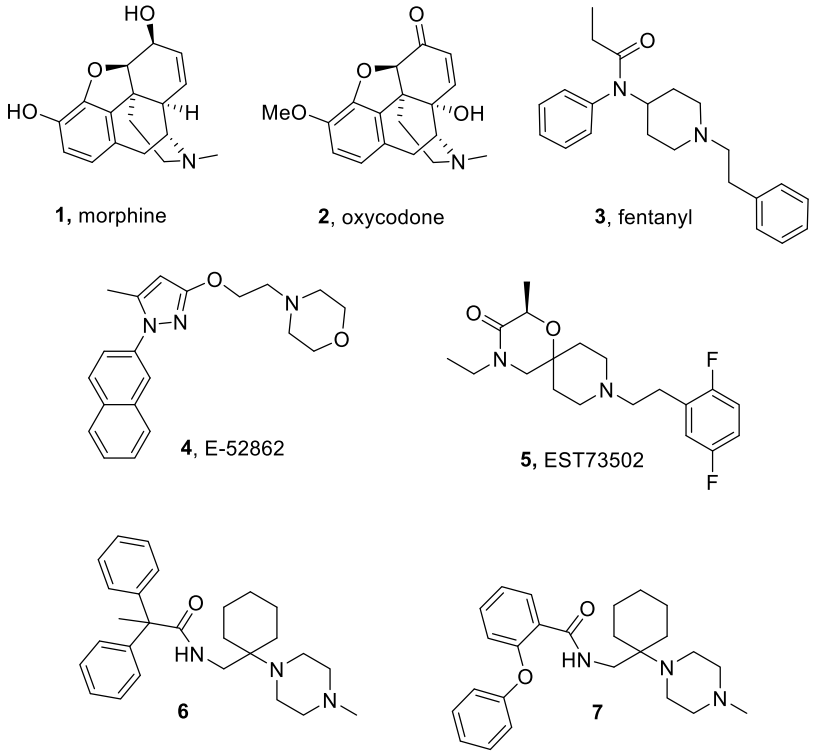

Figure 1. Structures of MOR agonists (**1**–**3**), σ_1R antagonist (**4**), dual clinical candidate (**5**), and dual HTS hits (**6** and **7**).

Table 1. Exploration of Substituents in R^1, $R^{1'}$, and R^2

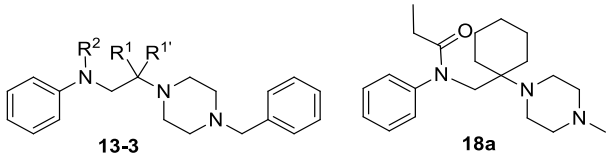

Comp	R^1, $R^{1'}$	R^2	K_i MOR[a] (*h*, nM)	EC_{50} MOR[b] (*h*, nM)	E_{max} MOR[c] (%)	K_i σ_1R[d] (*h*, nM)	clog *P*
2			12 ± 3	17 ± 9	100	>10000	0
4			>10000	>10000		17 ± 7	3.9
6			297 ± 89	1167 ± 105	91	955 ± 217	4
7			1005 ± 319	4527 ± 559	74	699 ± 31	4.3
13-3	Me, Me	H	>1000	>10000		10 ± 1	4.8
15a	cyclohexyl	COEt	43 ± 3	158 ± 5	71	23 ± 1	6.4
15b	H, H	COEt	212 ± 70	515 ± 85	82	92 ± 27	4.4
15c	Me, Me	COEt	95 ± 41	299 ± 14	37	14 ± 3	5.1
15d	Me, Me	$COCH_2OCH_3$	>1000	1468 ± 107		48 ± 8	4.7
15e	cyclopropyl	COEt	2 ± 1	34 ± 1	62	42 ± 4	4.7
15f	cyclopropyl	$COCH_2OCH_3$	72 ± 20	>10000		54 ± 3	4.2
18a	cyclohexyl	COEt	>1000	>10000		496 ± 82	3.1

[a]Binding affinity (K_i) in an MOR binding assay using [^{3}H]-DAMGO as the radioligand. Each value is the mean ± SD of two determinations. [b]MOR functionality (EC_{50}) measuring cAMP on CHO-K1 cells. Each value is the mean ± SD of two determinations. [c]An efficacy of 100% is defined as the maximum effect induced by stimulation with DAMGO. It is provided for compounds showing EC_{50} below 1000 nM in the functional assay. [d]Binding affinity (K_i) to the human σ_1R in transfected HEK-293 membranes using [^{3}H](+)-pentazocine as the radioligand. Each value is the mean ± SD of two determinations.

such as E-52862 (**4**, Figure 1),[19,20] have also proven the involvement of the σ_1R in pain. Compound **4**, both preclinically[21] and clinically,[22] has shown evidence that the σ_1R would be a good target for enhancing MOR analgesia without affecting opioid-induced side effects.

As a first approach to the development of dual σ_1R antagonists and MOR agonists, we recently reported a series that was conceived through a merging approach of the two target pharmacophores, considering common features in their structures.[23,24] From this research program, compound EST73502 (**5**, Figure 1) was selected as a clinical candidate[25] for the treatment of pain.

As a complementary strategy in this promising research line, a high-throughput screening (HTS) campaign was undertaken, leading to the identification of two dual hits, **6** and **7** (Figure 1), with the common structure *N*-((1-(4-methylpiperazin-1-

https://doi.org/10.1021/acs.jmedchem.1c00417
J. Med. Chem. 2021, 64, 10139−10154

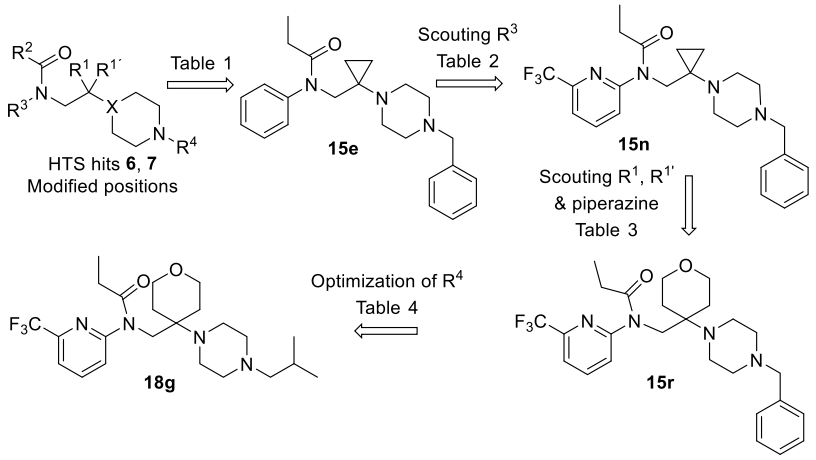

Figure 2. Modification sequence from **6** and **7** to **18g**.

Scheme 1. Synthesis Route of Compounds 18 Starting from Substituted Piperazines 9 and Ketone 8[a]

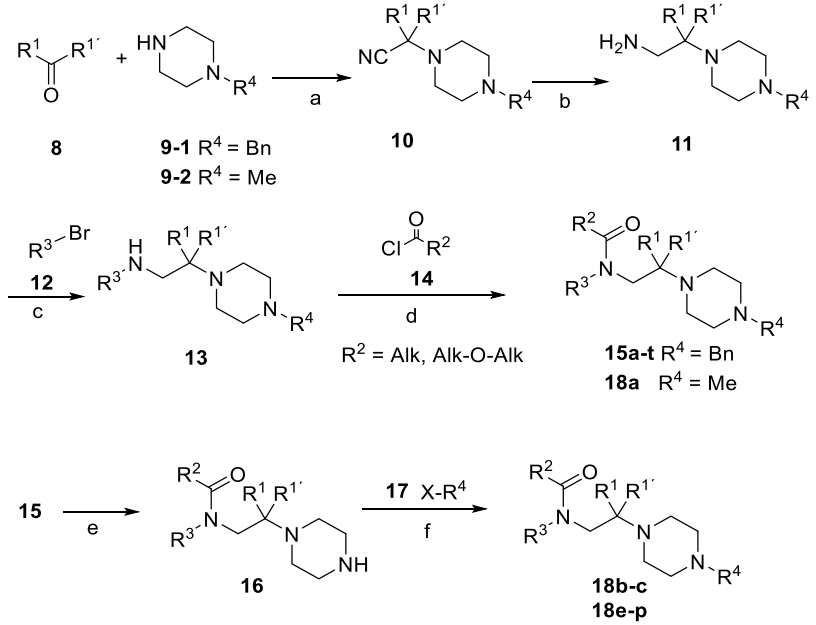

[a]Reagents and conditions: (a) $Na_2S_2O_5$, H_2O, KCN, rt, 2 days; (b) $LiAlH_4$, Et_2O, 0 °C to rt, 1 h; (c) $Pd_2(dba)_3$, BINAP, ^tBuOK, THF, 50 °C, overnight; (d) TEA, DCM, rt, 0.5 h or DIPEA, DCE, 85 °C, 0.5 h; (e) NH_4HCO_2, 20% Pd/C, MeOH, 65 °C, 1 h; and (f) K_2CO_3, acetonitrile, 50 °C, overnight or DIPEA, KI, acetonitrile, MW, 80 °C, 1 h.

yl)cyclohexyl)methyl)amide and an incipient dual affinity (see Table 1). We report here the synthesis and SAR studies (structure−activity relationships) of a new series of piperazinylcycloalkylmethyl-*N*-arylpropionamides[26] that were designed based on these initial dual HTS hits. Figure 2 shows a summary of the modifications performed from hits **6** and **7** that led to the identification of the lead compound **18g**.

CHEMISTRY

Schemes 1−4 depict the synthesis of the compounds described herein. Starting from substituted piperazines **9**, a convenient route was designed to prepare final compounds **15** and **18** (Scheme 1). The Strecker reaction[27,28] of **9** with ketone **8** led to nitrile intermediates **10**. Reduction of the nitrile group to amines **11** and subsequent arylation under Buchwald−Hartwig coupling conditions with the appropriate bromoaryls **12** led to arylamines **13** in good yields. Finally, *N*-acylation with the corresponding acid chlorides **14** provided the benzyl (**15a-t**) and methyl (**18a**) derivatives. Alternative groups in R^4 (Table 4) were introduced by cleaving the benzyl group of **15** followed by *N*-alkylation of **16** with the corresponding alkyl halides **17** to give final compounds **18**. Compound **19** (Table 3) was prepared following the synthetic route depicted in Scheme 1, but using 2-benzyloctahydropyrrolo[3,4-*c*]pyrrole instead of 1-benzylpiperazine **9-1**.

For compounds **18** bearing a hydroxyl group in the *N*-alkyl chain in R^4, the final derivatization from compound **16** was performed, as depicted in Scheme 2. Opening of epoxide **20a** with piperazine **16a** provided a reaction mixture of regioisomers that was purified by preparative high-performance liquid chromatography (HPLC) to yield compounds **18d** and **18d′** as racemates. A similar reaction of amine **16a** with epoxide **20b** provided exclusive attack on the unsubstituted epoxide position to give compound **18q**.

https://doi.org/10.1021/acs.jmedchem.1c00417
J. Med. Chem. 2021, 64, 10139−10154

Table 2. Exploration of Aryl Groups in R^3

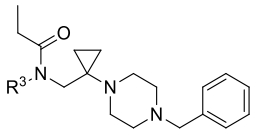

Comp	R^3	K_i MOR[a] (*h*, nM)	EC_{50} MOR[b] (*h*, nM)	E_{max} MOR[c] (%)	K_i σ_1R[d] (*h*, nM)	cLog*P*	hERG[e] IC_{50} (μM)	HLM[f] Cl_{int} (μL/min/mg prot)
15g	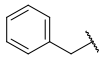	437 ± 61	>10000	-	8 ± 2	4.7	NT[g]	NT[g]
15h		9 ± 5	35 ± 9	48	175 ± 33	4	>10	95.7
15i		9 ± 3	73 ± 15	42	17 ± 2	4.7	2.6	77.6
15j	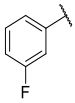	28 ± 7	12 ± 2	72	13 ± 3	4.8	1.2	135.7
15k		8 ± 5	39 ± 13	39	89 ± 29	3.2	NT[g]	NT[g]
15l		33 ± 8	24 ± 5	44	75 ± 10	3.2	>10	90.5
15m		32 ± 5	28 ± 3	57	36 ± 9	4.2	NT[g]	267.5
15n	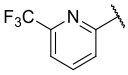	6 ± 4	32 ± 5	79	8 ± 1	4.2	3.5	111.2

[a]Binding affinity (K_i) in an MOR binding assay using [^{3}H]-DAMGO as the radioligand. Each value is the mean ± SD of two determinations. [b]MOR functionality (EC_{50}) measuring cAMP on CHO-K1 cells. Each value is the mean ± SD of two determinations. [c]An efficacy of 100% is defined as the maximum effect induced by stimulation with DAMGO. It is provided for compounds showing EC_{50} below 1000 nM in the functional assay. [d]Binding affinity (K_i) to the human σ_1R in transfected HEK-293 membranes using [^{3}H](+)-pentazocine as the radioligand. Each value is the mean ± SD of two determinations. [e]Whole-cell patch clamp hERG blockade. [f]Intrinsic clearance in human liver microsomes as a measure of metabolic stability, obtained as described in ref 33. [g]Not tested.

Although Scheme 1 could be of general application, in the case where R^1 and $R^{1'}$ are di-H, di-methyl, or spirocyclopropyl groups, some variations were used for the preparation of intermediates **13** (Scheme 3), which were then acylated to compounds **15** as described in Scheme 1. The unsubstituted derivative **13-2** was prepared by the acylation of **9-1** with chloroacetyl chloride, subsequent arylation of **21** with aniline (**22**), and final amide reduction of **23**. The synthesis of **13-3** involved alkylation of **9-1** with ethyl 2-bromo-2-methylpropanoate under microwave irradiation. Ester saponification to give carboxylic acid **24**, conventional amide coupling with aniline, and final reduction with alane (aluminum hydride) afforded intermediate **13-3**. Cyclopropyl derivatives **13-4** were synthesized following a strategy of piperazinyl cyclization. Treatment of diol **25** with thionyl chloride provided the dichloroethyl derivative **26**, which was cyclized with ethyl 1-aminocyclopropanecarboxylate and hydrolyzed to afford the key carboxylic intermediate **27**. Compound **27** was transformed into the primary carboxamide under amide coupling conditions with ammonium bicarbonate. Amide reduction and final Buchwald−Hartwig arylation with bromoaryls **12** provided intermediates **13-4**.

Piperidine analogue **36** was obtained as described in Scheme 4. The carbanion generated from tetrahydro-2*H*-pyran-4-carbonitrile **28** in the presence of lithium diisopropylamide (LDA) was added over Boc-protected 4-piperidone **29** to render intermediate **30**, which was then dehydrated with a Burgess reagent. The resulting tetrahydropyridine **31** was hydrogenated to the piperidine intermediate **32**. Boc-deprotection and introduction of the benzyl chain *via* reductive amination afforded piperidine **33**, which was reduced, arylated to install the R^3 substituent, and acylated to provide **36**, using similar conditions to those described in Scheme 1.

https://doi.org/10.1021/acs.jmedchem.1c00417
J. Med. Chem. 2021, 64, 10139−10154

Table 3. Heterocycloalkyl Groups in R^1 and $R^{1'}$ and Piperazine Replacement

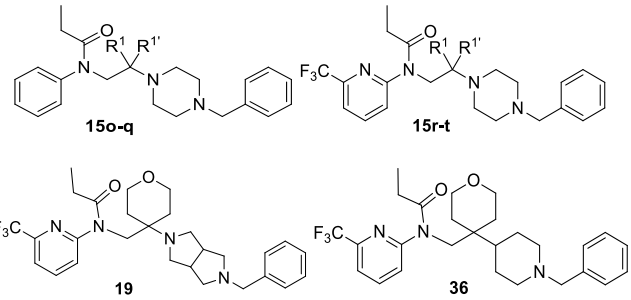

Comp	Tetrahydro pyranyl fine-tunning	K_i MOR[a] (*h*, nM)	EC_{50} MOR[b] (*h*, nM)	E_{max} MOR[c] (%)	K_i σ_1R[d] (*h*, nM)	cLog*P*	hERG[e] IC_{50} (μM)	HLM[f] Cl_{int} (μL/min/mg prot)
15o	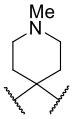	452 ± 88	738 ± 271	31	346 ± 39	4.2	>10	8.4
15p		107 ± 32	253 ± 16	56	42 ± 9	4	2.9	222.9
15q		14 ± 2	26 ± 24	46	21 ± 3	4.0	2.3	24.1
15r		5 ± 1	9 ± 2	85	30 ± 7	3.5	6.8	106.1
15s		6 ± 8	4 ± 1	99	47 ± 18	4.5	3.6	445.8
15t		37 ± 3	6 ± 2	100	70 ± 11	4.5	3.2	123.2
19		>1000	>1000	-	64 ± 9	3.4	3.4	NT[g]
36		82 ± 38	84 ± 7	77	60 ± 11	3.8	4.8	55.7

[a]Binding affinity (K_i) in an MOR binding assay using [^{3}H]-DAMGO as the radioligand. Each value is the mean ± SD of two determinations. [b]MOR functionality (EC_{50}) measuring cAMP on CHO-K1 cells. Each value is the mean ± SD of two determinations. [c]An efficacy of 100% is defined as the maximum effect induced by stimulation with DAMGO. It is provided for compounds showing EC_{50} below 1000 nM in the functional assay. [d]Binding affinity (K_i) to the human σ_1R in transfected HEK-293 membranes using [^{3}H](+)-pentazocine as the radioligand. Each value is the mean ± SD of two determinations. [e]Whole-cell patch clamp hERG blockade. [f]Intrinsic clearance in human liver microsomes as a measure of metabolic stability, obtained as described in ref 33. [g]Not tested.

RESULTS AND DISCUSSION

All synthetized compounds were tested in human σ_1R and MOR binding assays using [^{3}H]-(+)-pentazocine[29] and [^{3}H]-DAMGO[30] as radioligands, respectively. The MOR functional assay involves cyclic AMP (cAMP) measurement on CHO-K1 cells.[31] Potency (EC_{50}) as well as efficacy (E_{max}) data are provided in Tables 1−4. Compounds with E_{max} above 80% are assigned as full agonists, while compounds with E_{max} below 80% are considered as partial agonists at the MOR. Compounds binding to the MOR but with an antagonist profile at the MOR (inactive in the functional assay or E_{max} below 20%) were not identified in our series, suggesting a functional, scaffold-related agonistic bias of piperazinylcycloalkylmethyl propionamides. The functionality *versus* the σ_1R was not generally studied since there is not an efficient screening functionality assay due to the unique ligand-regulated molecular chaperone nature of the target.

The selectivity of the dual active compounds identified was evaluated at 1 μM in a small selectivity panel as previously described.[23] The best lead compounds **18e**, **18g**, and **18k** described here were selective *versus* this panel (% inhibition lower than 50% at 1 μM).

A significant challenge in the design of dual compounds is getting suitable drug-like properties as the space for optimization is narrowed by the need of maintaining both

https://doi.org/10.1021/acs.jmedchem.1c00417
J. Med. Chem. 2021, 64, 10139−10154

Table 4. Optimization of Piperazine Substituents R^4

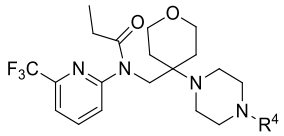

Comp	R^4	K_i MOR[a] (*h*, nM)	EC_{50} MOR[b] (*h*, nM)	E_{max} MOR[c] (%)	K_i σ_1R[d] (*h*, nM)	*c*Log*P*	hERG[e] IC_{50} (μM)	HLM[f] Cl_{int} (μL/min/mg prot)
16a		209 ± 70	1237 ± 142	-	>1000	0.8	>10	NT[g]
18b	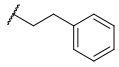	19 ± 4	>10000	-	35 ± 9	2.4	NT[g]	NT[g]
18c		83 ± 21	142 ± 60	77	34 ± 7	3.8	>10	111.7
18d		171 ± 92	972 ± 150	96	667 ± 149	2.7	NT[g]	NT[g]
18d'	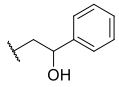	65 ± 35	>1000	-	479 ± 96	1.3	NT[g]	NT[g]
18e		220 ± 73	180 ± 55	54	231 ± 45	1.4	>10	9.4
18f		73 ± 24	510 ± 175	55	147 ± 22	1.9	2.2	14.5
18g		251 ± 141	183 ± 111	74	108 ± 46	1.7	>10	17.8
18h	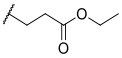	279 ± 99	598 ± 104	43	152 ± 33	1.2	NT[g]	NT[g]
18i		754 ± 180	720 ± 274	41	258 ± 80	0.5	NT[g]	NT[g]
18j	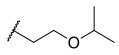	28 ± 7	53 ± 3	79	54 ± 13	1.2	>10	36.2
18k	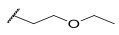	168 ± 53	210 ± 61	62	132 ± 75	0.9	>10	25.2
18l	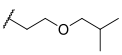	49 ± 12	30 ± 6	93	60 ± 10	1.8	9.5	121.6
18m	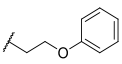	46 ± 18	133 ± 23	74	51 ± 16	2.3	2.3	148.6
18n	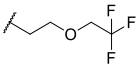	157 ± 68	314 ± 41	67	53 ± 11	1.2	8.7	58.2
18o	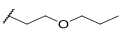	137 ± 72	86 ± 15	77	27 ± 8	1.4	3.4	49.5
18p	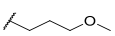	267 ± 93	>10000	-	387 ± 50	0.7	>10	11.2
18q		>1000	869 ± 73	75	110 ± 55	0.5	>10	NT[g]

[a]Binding affinity (K_i) in an MOR binding assay using [^{3}H]-DAMGO as the radioligand. Each value is the mean ± SD of two determinations. [b]MOR functionality (EC_{50}) measuring cAMP on CHO-K1 cells. Each value is the mean ± SD of two determinations. [c]An efficacy of 100% is defined as the maximum effect induced by stimulation with DAMGO. It is provided for compounds showing EC_{50} below 1000 nM in the functional assay. [d]Binding affinity (K_i) to the human σ_1R in transfected HEK-293 membranes using [^{3}H](+)-pentazocine as the radioligand. Each value is the mean ± SD of two determinations. [e]Whole-cell patch clamp hERG blockade. [f]Intrinsic clearance in human liver microsomes as a measure of metabolic stability, obtained as described in ref 33. [g]Not tested.

https://doi.org/10.1021/acs.jmedchem.1c00417
J. Med. Chem. 2021, 64, 10139−10154

Scheme 2. Derivatization Route of Compounds 18 Starting from Compound 16a[a]

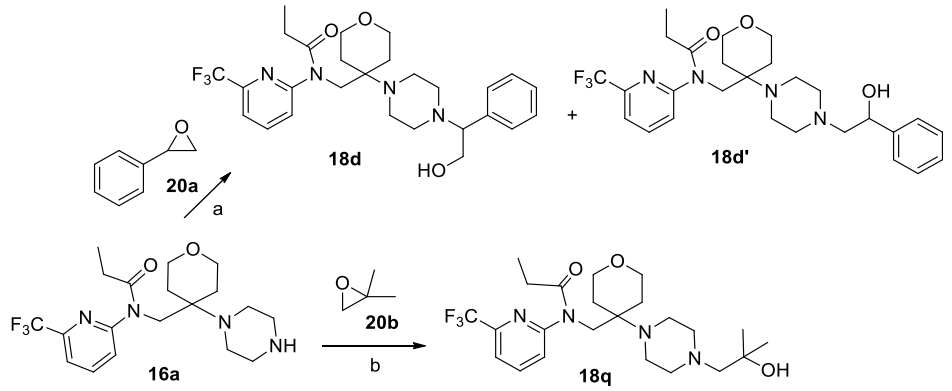

[a]Reagents and conditions: (a) EtOH, 70 °C, overnight; (b) TEA, MeOH, 75 °C, 3 h.

Scheme 3. Synthetic Routes of Intermediates 13[a]

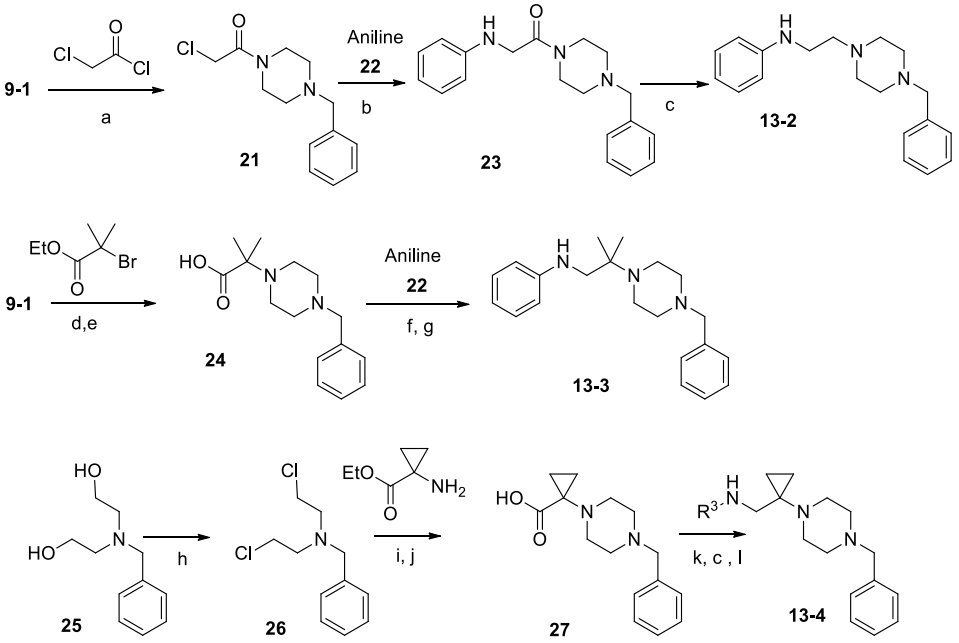

[a]Reagents and conditions: (a) DCM, rt, 0.5 h; (b) TEA, NaI, DMF, rt, overnight; (c) $LiAlH_4$, THF, 0 °C to 65 °C, overnight; (d) TEA, EtOH, MW, 150 °C, 3.5 h; (e) NaOH, MeOH, 65 °C, 6 h; (f) HOBt, EDC, DMF, TEA, rt, overnight; (g) alane solution in THF, 0 °C, 1.5 h; (h) thionyl chloride, DCM, rt, overnight; (i) $NaHCO_3$, EtOH, 80 °C for 4 h, then overnight at rt; (j) KOH, EtOH, 120 °C, 5 h; (k) ammonium bicarbonate, HATU, TEA, DMF, 0 °C to rt, 2 days; and (l) R^3Br (**12**), $Pd_2(dba)_3$, BINAP, ^tBuOK, THF, 50 °C, overnight.

activities.[32] Metabolic stability measured as the intrinsic clearance in human liver microsomes was obtained for the dual compounds,[33] and we also assayed the blockade of the human ether-a-go-go-related gene (hERG),[34] whose inhibition has been a constant concern in our previous σ_1R programs.[14] The results of these tests are shown in Tables 2–4.

As mentioned before, screening of our internal compound library led to the identification of the dual hits **6** and **7** (Figure 1 and Table 1) with an incipient submicromolar dual affinity. Starting from the common structure of *N*-((1-(4-methylpiperazin-1-yl)cyclohexyl)methyl) amide, we decided to preserve the methylpiperazin-1-ylcycloalkyl moiety and modify the nature of the amide substitution. The acylarylamine present in fentanyl (**3**) was installed instead of the bulky amide group present in the HTS hits. The first synthesized compound **18a** slightly improved the σ_1R affinity but was devoid of MOR activity. In parallel, we prepared compound **15a**, in which the methyl group was replaced by a benzyl group, which usually gives good σ_1R affinities as a hydrophobic group is required at a suitable distance from the basic amine, as described in the new σ_1R model[35] built using the Langer pharmacophore.[36] We were delighted to see that **15a** showed an improved σ_1R affinity, regaining at the same time MOR agonist functionality. However, it exhibited a very low metabolic stability (human Cl_{int} 67.9 μl/min/mg protein), which we reasoned could be attributed to its high clog *P*.

Exploration of smaller substituents in R^1 and $R^{1'}$ to decrease lipophilicity was first studied (Table 1). The unsubstituted **15b** was 5-fold less potent than **15a**, but the dimethyl (**15c**) and spirocyclopropyl (**15e**) derivatives showed a significant improvement. The hydrogen-bond-acceptor propionyl moiety in R^2 was proven necessary to interact with the MOR, as shown by the lack of activity of compound **13-3**. However, an additional heteroatom was not tolerated (**15d** and **15f**).

https://doi.org/10.1021/acs.jmedchem.1c00417
J. Med. Chem. 2021, 64, 10139−10154

Scheme 4. Synthetic Process of Piperidine Analogue 36[a]

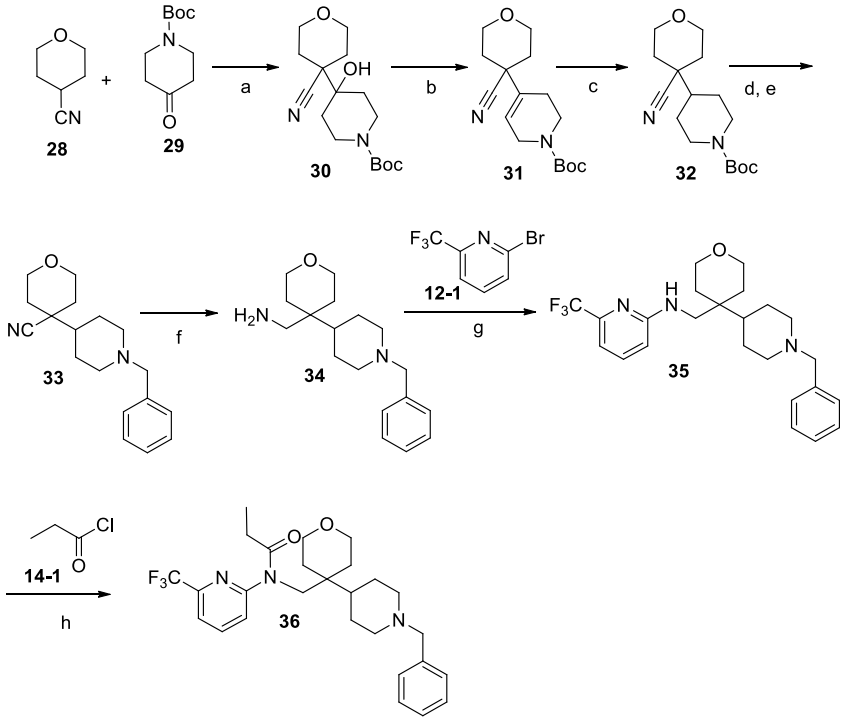

[a]Reagents and conditions: (a) LDA, THF, −78 °C, 2 h; (b) Burgess reagent, toluene, 90 °C, overnight; (c) H_2, Pd/C, EtOH, rt, overnight; (d) TFA, DCM, rt, 1 h; (e) benzaldehyde, $NaBH(OAc)_3$, THF, a few drops of AcOH, rt, overnight; (f) $LiAlH_4$, Et_2O; (g) $Pd_2(dba)_3$, BINAP, *t*BuOK, THF, 55 °C, overnight; and (h) TEA, DCM, rt, 0.5 h.

Among the initial compounds, propionamide **15e** with spirocyclopropyl substitution in R^1 and $R^{1'}$ displayed the best dual MOR and σ_1R affinities with potent partial MOR agonism. Despite its substantial decrease in lipophilicity *versus* that of **15a**, its metabolic stability was again quite low (human Cl_{int} 90.5 μL/min/mg protein), so additional efforts were focused on further decreasing clog *P* or avoiding potential metabolic hotspots.

We next explored the aryl substitution in R^3 over the most promising cyclopropyl derivative (Table 2). While the *N*-benzyl substituent had low affinity for the MOR (**15g**), *N*-phenyl significantly increased the affinity as well as agonist potency, keeping also the affinity for the σ_1R (compounds **15e** and **15h−j**). Introduction of fluorine atoms (**15i** and **15j**) failed at improving the metabolic stability. A hydroxyl group in the *ortho* position (**15h**) gave an improvement in hERG inhibition but with diminished σ_1R affinity and metabolic stability. Introduction of the three possible pyridyl isomers in R^3 was also explored. Only the 2-pyridyl derivative (**15k**) maintained the desired affinity for both targets, while MOR affinity and functionality worsened for the 3- and 4-pyridyl analogues (data not shown). Many substituents were tested at different positions of the 2-pyridyl group, and the derivatives containing a trifluoromethyl or fluorine group in the *ortho* position (**15l−n**) were particularly interesting in terms of their good dual activities. Unfortunately, the best compound (**15n**) was not optimal regarding metabolic stability and hERG inhibition.

With the key learnings achieved at this point of the SAR study, we considered further optimization of R^1 and $R^{1'}$ because it is well known that cycloalkyl motifs are prone to suffer oxidation by CYP3A4,[37,38] which could be the cause of the poor human metabolic stability observed so far. The data reported in Table 3 show that introduction of polarity in R^1 and $R^{1'}$ led to greatly improved metabolic stability for piperidyl (**15o**) and tetrahydropyranyl (**15q**) analogues, although at the expense of dual affinity in the case of **15o**. Other analogues were prepared, maintaining a 6-(trifluoromethyl)-2-pyridinyl group in position R^3. Dimethyl (**15t**) substitution in the 2-position of the tetrahydropyran ring and changing the oxygen atom with a sulfur atom to give tetrahydrothiopyranyl derivative **15s** were tolerated by both targets but were clearly detrimental regarding hERG inhibition.

Replacement of the piperazine by a piperidine ring (**36**) maintained the duality, suggesting that N4 of the piperazine nucleus was the positive ionizable feature required by both targets. Surprisingly, changing the piperazine with bicycle octahydropyrrolo[3,4-*c*]pyrrole (**19**) led to a complete loss of MOR activity.

In the following optimization round, we set out to explore different alternatives to the benzyl moiety in R^4 while maintaining the best substituents in the remaining positions (Table 4). As expected, and in line with the data obtained with compound **18a**, the unsubstituted piperazine **16a** was poorly active, while the phenethyl derivative **18b** lost MOR agonism. One of the strategies for detuning hERG inhibition is the generation of steric bulk near the basic amine or reducing the planarity.[39] With this aim, branched analogues were prepared. The α-methylbenzyl derivative **18c** showed a favorable hERG inhibition result, but it had poor metabolic stability in humans. The decrease in clog *P* by the introduction of a 2-hydroxy group to **18c** (**18d**) provided an impairment in the σ_1R affinity, a result not totally unexpected in view of the hydrophobicity of the σ_1R. Propyl (**18e**) and butyl (**18f**) derivatives showed a

https://doi.org/10.1021/acs.jmedchem.1c00417
J. Med. Chem. 2021, 64, 10139−10154

Table 5. PK Parameters of Compound 18g in Mice[a]

route	dose(mg/kg)	$t_{1/2}$ (h)	C_{max} (ng/mL)	t_{max} (h)	AUC_{0-t} (ng·h/mL)	AUC (ng·h/mL)	Cl (l/h/kg)	V_{ss} (l/kg)	F (%)
po	10	n.c.	130	0.5	122	n.c.			13
ip	40	0.6	11319	0.08	5953	5955			>100
iv	1	0.4			92	93	10.8	2.9	

[a]n.c.: not calculable (extrapolated AUC >20%).

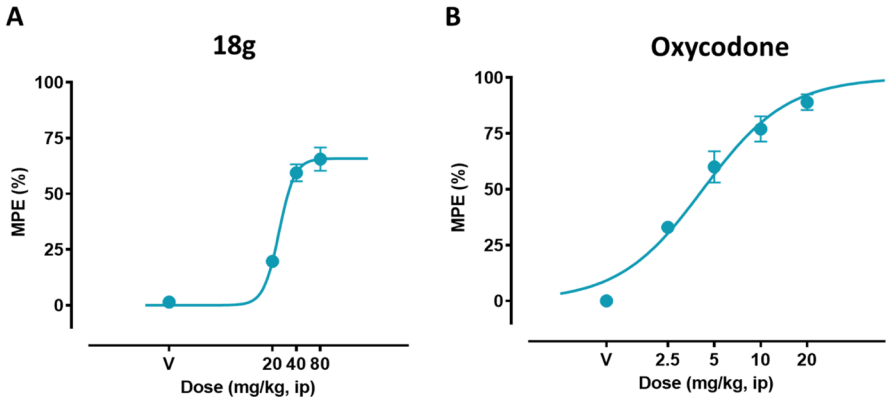

Figure 3. Dose−response antinociception curve in the paw pressure test of **18g** (A) and oxycodone (B) administered in male CD1 mice after ip administration. Each point and vertical line represent the mean ± S.E.M of the maximum possible effect percentage of the effect (n = 6−8 per group).

significant decrease in σ_1R affinity and MOR agonism in comparison with the parent benzyl (**15r**), although **18e** showed improved hERG inhibition and metabolic stability. A slight increase in the hydrophobicity in compound **18g** provided a 2-fold improvement in σ_1R affinity, with a moderate metabolic stability and hERG IC_{50} above 10 μM. Introduction of oxygen atoms in the alkyl chains was detrimental in the ester (**18h**) and hydroxyl (**18q**) derivatives but was tolerated in the case of ethers, with the exception of **18i**. Some of them displayed interesting dual affinities for the primary targets with potent MOR agonism (**18j**, **18l**, **18m**, and **18o**) but were still suboptimal regarding metabolic stability.

Overall, compounds **18e**, **18g**, and **18k** emerged as some of the best derivatives, showing good affinity for primary targets, balanced in the case of **18g** to a higher σ_1R affinity. Although the optimal ratio for the σ_1R and MOR *in vitro* affinities is difficult to establish, a predominant affinity for the MOR would not be desirable because it would increase the likelihood for opioid-related adverse effects and, importantly, it would mask the σ_1R antagonism enhancement of opioid analgesia. In fact, compound **4** showed the best results when combined with low doses of morphine: E-52862, 40 mg/kg and morphine, 2.5−5 mg/kg.[15]

Compound **18g** was selected for further *in vitro* and *in vivo* characterizations. Regarding the selectivity, exhaustive *in vitro* characterization of compound **18g** revealed the lack of significant affinity (inhibition % at 10 μM < 50%) for 180 molecular targets (receptors, transporters, ion channels, and enzymes),[40] except for the σ_2R (K_i 413 nM). Phenytoin binding experiments[41] showed an antagonistic behavior for the σ_1R, while experiments with β-funaltrexamine[31] confirmed the partial agonism at the MOR (results not shown). Additionally, compound **18g** did not show *in vitro* cytotoxic potential at 100 μM in HepG2 cells, both in the neutral red uptake and in the MTT [3-(4,5-dimethylthiazol-2-yl)-2,5-diphenyltetrazolium bromide] assays.[42] It was also devoid of genotoxic potential in the SOS/umu and Ames bacterial mutation assays.[43]

Compound **18g** exhibited an adequate physicochemical profile, with moderate basicity (pK_a 8.9) and lipophilicity (experimental log P 3.7, log $D_{7.4}$ 2.2) and good solubility in the whole physiologically meaningful pH range (thermodynamic solubility > 0.5 mg/mL at pH 7.4 and pH 2). This, together with its good permeability in Caco-2 cells ($P_{appA\text{-}to\text{-}B}$ 169 nm/s), predicts a good oral (po) absorption in humans.[44] It also complied with Lipinski's rules and presented a good value (4.8) in the central nervous system (CNS) multi-parameter optimization algorithm developed by Wager *et al.*[45] as a holistic approach for the prediction of good ADME (absorption, distribution, metabolism, and excretion) and safety attributes in the case of CNS-directed compounds.

The PK behavior of **18g** was evaluated in mice after po, intraperitoneal (ip), and intravenous (iv) administration of single doses of 10, 40, and 1 mg/kg, respectively, and comparative data are outlined in Table 5. The po plasma exposure was not very high, but the exposure after ip administration of 40 mg/kg was high, and it was selected as a representative dose for establishing initial PK/pharmacodynamics relationships as discussed below. Furthermore, the CNS distribution of **18g** was evaluated in rats as a representative rodent species, where it showed a similar exposure in the plasma and brain (AUC 2811 and 2434 ng·h/mL in the plasma and brain, respectively, a brain-to-plasma ratio of 0.9) after ip administration of 40 mg/kg.

Compound **18g** was evaluated for its *in vivo* activity in the mouse paw pressure test of acute pain in CD1 mice (n = 6−8 per group). After ip administration, **18g** showed a dose−response analgesic effect, reaching a maximum of 66 ± 5.2% and an ED_{50} of 24 ± 0.78 mg/kg (Figure 3). The ip administration of oxycodone also induced a dose−response effect, reaching a maximum of 89 ± 3.5% and an ED_{50} of 4 ± 0.4 mg/kg.

The antinociceptive activity of **18g** was also evaluated following repeated/subchronic administration for 10 days in the partial sciatic nerve ligation (PSNL) model of neuropathic

https://doi.org/10.1021/acs.jmedchem.1c00417
J. Med. Chem. 2021, 64, 10139−10154

pain in CD1 male mice in comparison to that of oxycodone (**2**). Mechanical hypersensitivity (mechanical allodynia) was evaluated as a neuropathic pain-related behavior, as described in the Supporting Information. Repeated administration of compound **18g** (20 mg/kg, ip) and oxycodone (compound **2**, 1.25 mg/kg, ip) showed that both **18g** and **2** attenuated mechanical allodynia induced by PSNL, reaching maximal effects of 96 ± 13.9 and 41 ± 9.1%, respectively. Interestingly, repeated administration of **18g** twice daily over 10 days did not induce tolerance but an increased antinociceptive effect, with the analgesic effect being higher at day 22 than that at day 13 (p = 0.0052) (Figure 4).

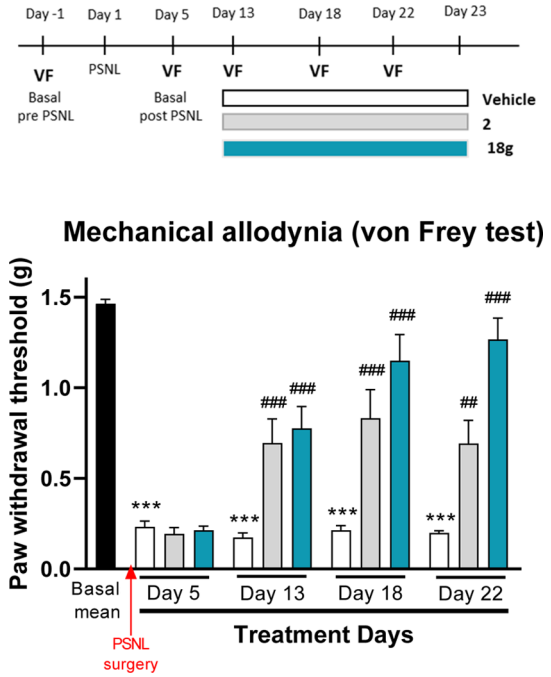

Figure 4. Effect of **18g** (blue bars) or oxycodone (**2**, gray) in comparison to the vehicle (white) on PSNL-induced mechanical allodynia in male CD1 mice. Compounds **18g** (20 mg/kg) and **2** (1.25 mg/kg) were systemically (ip) administered twice daily for 10 days. Each bar and vertical line represent the mean ± S.E.M. paw withdrawal threshold (n = 6−12 per group). ***p < 0.001 *versus* basal mean; ##p < 0.01; and ###p < 0.001 *versus* each vehicle group (one-way ANOVA, followed by Tukey's test).

Intestinal transit reduction (as a surrogate of constipation) was evaluated in CD1 mice by measuring the percentage of the distance traveled by the charcoal meal *versus* the total length of the small intestine after drug administration and comparing to that of the control group that received the vehicle. Figure 5 shows that, at the doses used, **18g** and **2** induced similar antinociceptive effects (**18g** = 59.4 ± 8.3%, **2** = 77 ± 5.7%, p = 0.10), whereas they produced a differentiated effect on the intestinal transit. Compound **18g** did not reduce the intestinal transit (p = 0.35 *vs* vehicle), whereas oxycodone produced significant constipation in comparison with the vehicle group (p = 0.01 *vs* vehicle).

CONCLUSIONS

A new series of piperazinyl-cycloalkylmethyl-*N*-aryl-propionamide derivatives as dual ligands for the MOR and σ_1R is reported. This dual approach aims at enhancing opioid analgesia by additionally targeting the σ_1R, which may provide an increased effect in nociceptive and neuropathic analgesia without affecting opioid-induced side effects. Starting from two HTS dual hits, significant improvements in dual affinities were achieved after the first round of modifications in the amide, cyclohexyl, and methyl-piperazine groups of the initial hits structure, as exemplified by derivatives **15a** and **15e**. Since these compounds exhibited very low metabolic stability, a hit-to-lead program was initiated to decrease clog P, maintaining dual activities and also dealing with hERG inhibition, which emerged as an additional challenge in the optimization of this series. The best compounds identified (**18e**, **18g**, and **18k**) showed good dual affinities, low hERG inhibition, and acceptable metabolic stability. Compound **18g** was selected for further characterization and demonstrated analgesic activity in acute and chronic pain mice models, with less opioid-induced tolerance and constipation than oxycodone. These results place the **18g** lead compound and the chemical series described herein as potential subjects for a lead optimization program to develop a backup compound for candidate EST73502 currently in clinical trials.

EXPERIMENTAL SECTION

Unless otherwise noted, all materials were obtained from commercial suppliers and used without further purification. Reference compounds used in biological assays were obtained from the following vendors: oxycodone hydrochloride (**2**) was obtained from Macfarlan Smith Ltd (UK); E-52862 (**4**) was obtained as previously described;[14] and HTS compounds **6** and **7** were acquired from Cerep.

Flash chromatography was performed on a Teledyne Isco CombiFlash RF system with disposable columns. ^{1}H spectra were recorded on an Agilent Mercury 400 MHz spectrometer fitted with a

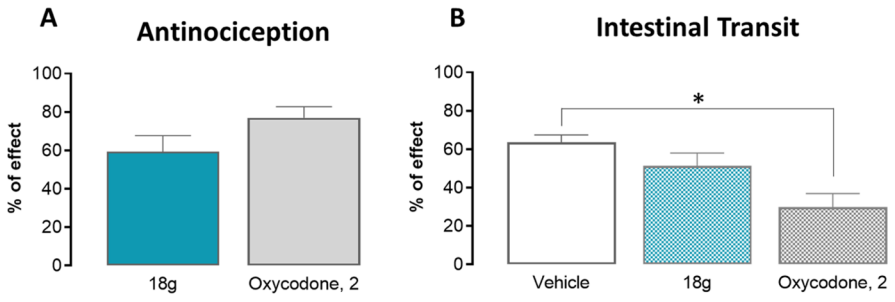

Figure 5. Effect of **18g** (40 mg/kg, ip, blue bars) or oxycodone (**2**) (10 mg/kg, ip, gray bars) on the analgesic response (paw pressure test) (A) and on the intestinal transit measured in the charcoal test (B) in male CD1 mice after drug administration. Each bar and vertical line represent the mean ± S.E.M. percentage of effect (n = 4−14 per group). *p < 0.05 comparing with the vehicle (HPMC 0.5%, white bar; one-way ANOVA, followed by Tukey's test).

https://doi.org/10.1021/acs.jmedchem.1c00417
J. Med. Chem. 2021, 64, 10139−10154

5 mm ATB 1H/19F/X probe with a 2 H lock in deuterated solvents. Chemical shifts (δ) are in parts per million. Commercially available reagents and solvents (HPLC grade) were used without further purification for all the analytical tests. Analytical HPLC−mass spectrometry (HPLC-MS) for all final compounds and intermediates were performed on a Waters H-Class-ZQ MS system. A reverse-phase Acquity C18 BHE column was used (2.1 × 5 mm, 1.7 μm) under the following conditions: gradient 0.3 min in 98% A, 98% A to 5% A in 2.52 min, and isocratic 1.02 min in 5% A (A = 10 mM ammonium bicarbonate and B = acetonitrile); injection volume: 2 μL; flow: 0.61 mL/min; and temperature: 35 °C. UV spectra were recorded from 195 to 315 nm using a Waters Acquity photodiode array detector. Mass spectra were obtained over the range m/z 100−800 by electrospray ionization (ESI) in positive and negative modes using a Waters ZQ Single Quadrupole. Data were integrated and reported using Waters MassLynx software. All final compounds displayed a purity equal or higher than 95%, as determined by said methods, except for **15a**, whose purity was 85%. Accurate mass measurements were carried out using an Agilent 6540 UHD high-resolution mass spectrometer quadrupole time-of-flight system and obtained by ESI in the positive mode. Data were acquired and processed using MassHunter software. All compounds active in biological assays were electronically filtered for structural attributes common to pan assay interference compounds and were found to be negative.[46]

Physicochemical properties of compounds were determined as previously described.[24,47] All compounds have been named using ChemBioDraw Ultra 12.0.2.

General Procedures for the Synthesis of Piperazinyl-cycloalkylmethyl-*N*-aryl-propionamide Derivatives 15 and 18. *N-((4-(4-Benzylpiperazin-1-yl)tetrahydro-2H-pyran-4-yl)-methyl)-N-(6-(trifluoromethyl)pyridin-2-yl)propionamide (**15r**). Step 1.* In a 2 L round-bottomed flask, dihydro-2*H*-pyran-4(3*H*)-one (**8-1**, 10.8 g, 107.8 mmol) was dissolved in water (500 mL) along with sodium metabisulfite (10.2 g, 54 mmol).[48] The mixture was allowed to stir at room temperature (rt) for 1.5 h, and then, benzylpiperazine (**9-1**, 19 g, 108 mmol) was added. The mixture was stirred for 2 h, and potassium cyanide (11.2 g, 173 mmol) was added to the reaction mixture. After stirring at rt for 2 days, the solid formed was filtered and dried to give 4-(4-benzylpiperazin-1-yl)tetrahydro-2*H*-pyran-4-carbonitrile (**10-1**) as a white solid (27.8 g, 90% yield). ^{1}H NMR (400 MHz, $CDCl_3$): δ 7.35−7.28 (m, 4H), 7.31−7.22 (m, 1H), 4.09−3.91 (m, 2H), 3.65 (td, J = 2.1, 12.3 Hz, 2H), 3.52 (s, 2H), 2.75−2.58 (m, 4H), 2.61−2.41 (m, 4H), 2.08 (dq, J = 2.5, 13.5 Hz, 2H), 1.72 (ddd, J = 4.5, 11.7, 13.2 Hz, 2H). HPLC-MS: m/z = 286 $[M + H]^+$.

Step 2. Compound **10-1** (2 g, 7 mmol) in tetrahydrofuran (THF)/Et_2O (40/20 mL) was added at 0 °C to a stirred solution of fresh lithium aluminum hydride in Et_2O (1 M, 14 mL, 14 mmol). The reaction was stirred at rt for 1 h, a few drops of an aqueous saturated solution of potassium sodium tartrate were added, and the mixture was stirred overnight at rt. Then, water and ethyl acetate were added, and the aqueous layer was separated and extracted several times with ethyl acetate. The organic layers were combined, dried over Na_2SO_4, filtered, and concentrated to give (4-(4-benzylpiperazin-1-yl)-tetrahydro-2*H*-pyran-4-yl)methanamine (**11-1**) as a solid (1.8 g, 88% yield). ^{1}H NMR (300 MHz, CD_3OD): δ 7.64−7.39 (m, 5H), 4.38 (s, 2H), 3.96−3.78 (m, 2H), 3.59 (t, J = 11.3 Hz, 2H), 3.47 (d, J = 11.9 Hz, 2H), 3.25 (s, 2H), 3.34−3.10 (m, 4H), 2.73 (t, J = 12.3 Hz, 2H), 2.02−1.84 (m, 2H), 1.53 (d, J = 13.7 Hz, 2H). HPLC-MS: purity 100%, m/z = 290 $[M + H]^+$.

Step 3. Compound **11-1** (3.6 g, 13.13 mmol), $Pd_2(dba)_3$ (1.14 g, 1.25 mmol), 2,2′-bis(diphenylphosphino)-1,1′-binaphthyl (BINAP, 0.93 g, 1.50 mmol), and ^{t}BuOK (2.8 g, 25.01 mmol) were dissolved in anhydrous THF (430 mL). 2-Bromo-6-(trifluoromethyl)pyridine (**12-1**, 2.96 g, 13.13 mmol) was added, and the reaction mixture was stirred under an inert atmosphere at 50 °C overnight. The solvents were evaporated, and the residue was dissolved in ethyl acetate and an aqueous saturated $NaHCO_3$ solution. The aqueous layer was extracted with ethyl acetate, and the combined organic layers were dried over Na_2SO_4, filtered, and concentrated. The crude product thus obtained was purified by flash chromatography on silica gel, gradient CH/ethyl acetate from (100:0) to (0:100), to give *N*-((4-(4-benzylpiperazin-1-yl)tetrahydro-2*H*-pyran-4-yl)methyl)-6-(trifluoromethyl)pyridin-2-amine (**13-1**) as a solid (3.53 g, 61% yield). ^{1}H NMR (400 MHz, CD_3OD): δ 7.50 (t, J = 7.9 Hz, 1H), 7.38−7.20 (m, 5H), 6.84 (d, J = 7.2 Hz, 1H), 6.71 (d, J = 8.5 Hz, 1H), 3.81 (ddd, J = 3.3, 7.6, 11.1 Hz, 2H), 3.64 (ddd, J = 3.4, 6.7, 11.0 Hz, 2H), 3.61 (s, 2H), 3.54 (s, 2H), 2.80 (t, J = 4.5 Hz, 4H), 2.58−2.45 (m, 4H), 1.90−1.76 (m, 2H), 1.62 (ddd, J = 3.3, 7.5, 12.4 Hz, 2H). HPLC-MS: purity 99%, m/z = 435 $[M + H]^+$.

Step 4. Propionyl chloride (**14-1**, 1.38 mL, 15.88 mmol) was added to a solution of compound **13-1** (2.3 g, 5.29 mmol) and *N*-ethyl-*N*-isopropylpropan-2-amine (DIPEA) (3.68 mL, 21.17 mmol) in dichloroethane under a nitrogen atmosphere. The reaction mixture was heated for 30 min at 85 °C, after which it was allowed to reach rt. The reaction mixture was diluted with dichloromethane (DCM) (25 mL), and water (25 mL) was added. The aqueous phase was acidified with 10% HCl, and the phases were separated. The organic phase was extracted with 10% HCl, and the aqueous phases were made alkaline with 20% NaOH while cooling. Ethyl acetate (10 mL) was added, the phases were separated, and the aqueous phase was extracted with ethyl acetate. The combined organic phases were dried over Na_2SO_4, filtered, and concentrated to give *N*-((4-(4-benzylpiperazin-1-yl)-tetrahydro-2*H*-pyran-4-yl)methyl)-*N*-(6-(trifluoromethyl)pyridin-2-yl)propionamide (**15r**) (2.45 g, 94% yield). ^{1}H NMR (400 MHz, CD_3OD): δ 8.13 (t, J = 6.9 Hz, 1H), 7.91−7.70 (m, 2H), 7.60−7.48 (m, 5H), 4.49−4.18 (m, 4H), 3.73 (ddt, J = 3.7, 6.3, 10.5 Hz, 2H), 3.68−2.67 (m, 10H), 2.25 (q, J = 7.3 Hz, 2H), 1.95−1.50 (m, 4H), 1.05 (t, J = 7.4 Hz, 3H). HPLC-MS: purity 99%. HRMS $[M + H]^+$ (diff ppm) 491.2645 (−3.38).

*N-((4-(4-Isobutylpiperazin-1-yl)tetrahydro-2H-pyran-4-yl)-methyl)-N-(6-(trifluoromethyl)pyridin-2-yl)propionamide (**18g**). Step 1.* Compound **15r** (427 mg, 0.87 mmol) was dissolved in MeOH (10 mL), and ammonium formate (246 mg, 3.91 mmol) and Pd/C (85 mg, 10% Wt) were added. The suspension was stirred under a N_2 atmosphere for 1 h at 65 °C. The reaction mixture was filtered through Celite, washed with MeOH, and concentrated to give ***N***-((4-(piperazin-1-yl)tetrahydro-2*H*-pyran-4-yl)methyl)-*N*-(6-(trifluoromethyl)pyridin-2-yl)propionamide (**16a**) (347 mg, 99% yield). ^{1}H NMR (400 MHz, $CDCl_3$): δ 8.42 (s, 1H), 7.97 (t, J = 8.0 Hz, 1H), 7.63 (d, J = 7.6 Hz, 1H), 7.42 (d, J = 8.1 Hz, 1H), 4.21 (s, 2H), 3.77−3.56 (m, 4H), 3.28−2.37 (m, 8H), 2.23 (q, J = 7.3 Hz, 2H), 1.74−1.59 (m, 2H), 1.52−1.39 (m, 2H), 1.09 (t, J = 7.3 Hz, 3H). HPLC-MS: purity 95%, m/z = 401 $[M + H]^+$.

Step 2. 1-Bromo-2-methylpropane (**17**, 39 μL, 0.36 mmol) was added to a solution of **16a** (80 mg, 0.2 mmol) and K_2CO_3 (83 mg, 0.6 mmol) in ACN (5 mL). The reaction mixture was stirred at 50 °C overnight and then was cooled down to rt. Ethyl acetate (10 mL) and saturated aqueous $NaHCO_3$ solution (10 mL) were added, and the phases were separated. The organic layer was dried over Na_2SO_4, filtered, and concentrated to give *N*-((4-(4-isobutylpiperazin-1-yl)tetrahydro-2*H*-pyran-4-yl)methyl)-*N*-(6-(trifluoromethyl)pyridin-2-yl)propionamide (**18g** free base) as an oil (67 mg, 73% yield). To a slurry of the previous free base (12 mg, 0.026 mmol) in ethyl acetate (1 mL), HCl (2 M solution in diethyl ether, 26 μL, 0.052 mmol) was added, and the mixture was stirred at rt for 0.5 h. The solids were dried in vacuo to give the **18g** HCl salt as a white solid (12.5 mg, 95% yield). ^{1}H NMR (400 MHz, D_2O): δ 8.25 (t, J = 7.9 Hz, 1H), 7.95 (d, J = 7.9 Hz, 1H), 7.86 (d, J = 8.1 Hz, 1H), 4.42 (s, 2H), 3.80 (dt, J = 4.2, 12.3 Hz, 2H), 3.75−3.30 (m, 8H), 3.25 (t, J = 11.1 Hz, 3H), 3.04 (d, J = 7.4 Hz, 2H), 2.25 (q, J = 7.3 Hz, 2H), 2.21−2.04 (m, 1H), 1.99−1.87 (m, 2H), 1.78 (d, J = 14.7 Hz, 2H), 0.99 (d, J = 6.6 Hz, 8H), 0.98 (t, J = 7.4 Hz, 6H). HPLC-MS: purity 99%. HRMS $[M + H]^+$ (diff ppm) 457.2783 (0.41).

*N-((4-(4-(2-Hydroxy-1-phenylethyl)piperazin-1-yl)tetrahydro-2H-pyran-4-yl)methyl)-N-(6-(trifluoromethyl)pyridin-2-yl)-propionamide (**18d**) and N-((4-(4-(2-Hydroxy-2-phenylethyl)-piperazin-1-yl)tetrahydro-2H-pyran-4-yl)methyl)-N-(6-(trifluoromethyl)pyridin-2-yl)propionamide (**18d′**).* A solution of **16a** (80 mg, 0.2 mmol) and 2-phenyloxirane (**20a**, 211 mg, 1.75

https://doi.org/10.1021/acs.jmedchem.1c00417
J. Med. Chem. 2021, 64, 10139−10154

mmol) in EtOH (5 mL) was heated at 70 °C in a sealed tube overnight. The reaction mixture was cooled to rt, and the solvent was evaporated. The residue was purified by preparative HPLC (Column X-Bridge C18, ACN: NH_4HCO_3 10 mM from 2:98 to 95:5, flow 20 ml/min, rt) to give *N*-((4-(4-(2-hydroxy-1-phenylethyl)piperazin-1-yl)tetrahydro-2*H*-pyran-4-yl)methyl)-*N*-(6-(trifluoromethyl)pyridin-2-yl)propionamide (**18d**) (13 mg, 13% yield) and *N*-((4-(4-(2-hydroxy-2-phenylethyl)piperazin-1-yl)tetrahydro-2*H*-pyran-4-yl)-methyl)-*N*-(6-(trifluoromethyl)pyridin-2-yl)propionamide (**18d′**) (6 mg, 6% yield). ^{1}H NMR (**18d**) (400 MHz, CD_3OD): δ 7.70 (t, J = 8.1 Hz, 1H), 7.57 (d, J = 8.1 Hz, 1H), 7.44−7.29 (m, 4H), 7.17 (d, J = 7.7 Hz, 2H), 4.24 (s, 2H), 3.89 (dd, J = 7.1, 11.1 Hz, 1H), 3.81−3.64 (m, 5H), 3.40−3.34 (m, 1H), 2.48 (d, J = 8.9 Hz, 4H), 2.13 (q, J = 7.4 Hz, 2H), 2.06−1.80 (m, 4H), 1.73 (tt, J = 4.6, 8.7 Hz, 2H), 1.55−1.38 (m, 2H), 0.99 (t, J = 7.4 Hz, 3H). HPLC-MS (**18d**): purity 100%. HRMS $[M + H]^+$ (diff ppm) 521.2754 (−3.65). ^{1}H NMR (**18d′**) (400 MHz, CD_3OD): δ 8.10 (ddq, J = 0.7, 7.7, 8.4 Hz, 1H), 7.76 (dd, J = 0.7, 7.7 Hz, 2H), 7.73 (dq, J = 0.7, 8.0 Hz, 2H), 4.74 (dd, J = 3.5, 9.2 Hz, 1H), 4.23 (s, 2H), 3.85−3.72 (m, 2H), 3.71−3.60 (m, 2H), 2.70−2.54 (m, 4H), 2.49 (dd, J = 9.2, 13.0 Hz, 1H), 2.31 (dd, J = 3.5, 13.0 Hz, 1H), 2.41−2.10 (m, 4H), 2.23 (q, J = 7.4 Hz, 2H), 1.81−1.65 (m, 2H), 1.59−1.43 (m, 2H), 1.05 (t, J = 7.4 Hz, 3H). HPLC-MS (**18d′**): purity 98%. HRMS $[M + H]^+$ (diff ppm) 521.2753 (−3.31).

*N-((4-(4-(2-Hydroxy-2-methylpropyl)piperazin-1-yl)tetrahydro-2H-pyran-4-yl)methyl)-N-(6-(trifluoromethyl)pyridin-2-yl)-propionamide (**18q**).* A solution of compound **16a** (500 mg, 1.25 mmol), 2,2-dimethyloxirane (243 mg, 3.37 mmol), and triethylamine (TEA) (379 mg, 3.74 mmol) in MeOH (20 mL) was stirred at 75 °C for 3 h. The solvent was concentrated in vacuum, and the residue was partitioned between DCM and water. The mixture was made alkaline with 20% NaOH, and the organic layer was separated, dried over Na_2SO_4, filtered, and concentrated. The crude residue was purified by flash chromatography on neutral alumine, gradient CH/ethyl acetate from (100:0) to (50:50), to give *N*-((4-(4-(2-hydroxy-2-methylpropyl)piperazin-1-yl)tetrahydro-2*H*-pyran-4-yl)methyl)-*N*-(6-(trifluoromethyl)pyridin-2-yl)propionamide (**18q**) as an oil (200 mg, 34% yield). ^{1}H NMR (400 MHz, CD_3OD): δ 8.11 (ddq, J = 0.7, 7.6, 8.2 Hz, 1H), 7.76 (dd, J = 0.7, 7.7 Hz, 1H), 7.73 (dq, J = 0.7, 8.1 Hz, 1H), 4.22 (s, 2H), 3.79 (ddd, J = 3.1, 7.9, 11.2 Hz, 2H), 3.64 (ddd, J = 3.3, 6.2, 10.9 Hz, 2H), 2.54 (t, J = 4.8 Hz, 4H), 2.35−2.21 (m, 4H), 2.23 (q, J = 7.4 Hz, 2H), 2.16 (s, 2H), 1.78−1.65 (m, 2H), 1.49 (ddd, J = 3.5, 7.9, 14.0 Hz, 2H), 1.13 (s, 9H), 1.05 (t, J = 7.4 Hz, 3H). HPLC-MS: purity 99%. HRMS $[M + H]^+$ (diff ppm) 473.2749 (−3.15).

*N-(2-(4-Benzylpiperazin-1-yl)ethyl)aniline (**13-2**). Step 1.* To a solution of chloroacetyl chloride (0.53 mL, 6.60 mmol) in dry DCM (25 mL) at 0 °C, 1-benzylpiperazine (**9-1**, 0.98 mL, 5.50 mmol) dissolved in dry DCM (25 mL) was added. The reaction mixture was stirred at rt for 0.5 h, the mixture was poured into cold H_2O (150 mL) and made alkaline with an aqueous saturated $NaHCO_3$ solution, and the phases were separated. The organic layer was dried over Na_2SO_4 and evaporated under reduced pressure to give 1-(4-benzylpiperazin-1-yl)-2-chloroethanone (**21**) as a yellow oil (1.46 g, quantitative yield). ^{1}H NMR (400 MHz, CD_3OD): δ 7.38−7.30 (m, 4H), 7.29−7.22 (m, 1H), 4.24 (s, 2H), 3.63−3.56 (m, 4H), 3.56 (s, 2H), 2.49 (dt, J = 5.2, 20.2 Hz, 4H). HPLC-MS: purity 94%, m/z = 253 $[M + H]^+$.

Step 2. Compound **21** (1.39 g, 5.5 mmol), TEA (2.3 mL, 16 mmol), and NaI (50 mg, 0.33 mmol) were dissolved in anhydrous dimethylformamide (DMF) (35 mL). Aniline (**22**, 0.51 mL, 6 mmol) was added, and the reaction was stirred at rt overnight. The mixture was partitioned between water and ethyl acetate/ethyl ether (1:1). The organic layer was washed with water, dried over Na_2SO_4, filtered, and concentrated to give 1-(4-benzylpiperazin-1-yl)-2-(phenylamino)ethanone (**23**) as a crude oil that was used in the following step without further purification (1.029 g, 60% yield). ^{1}H NMR (400 MHz, CD_3OD): δ 7.48−7.32 (m, 5H), 7.18−7.06 (m, 2H), 6.80−6.63 (m, 3H), 3.98 (s, 2H), 3.86 (s, 2H), 3.78−3.59 (m, 4H), 2.85−2.65 (m, 4H). HPLC-MS: m/z = 310 $[M + H]^+$.

Step 3. Compound **23** (0.5 g, 1.61 mmol) in THF (18 mL) was added at 0 °C to a stirred solution of fresh lithium aluminum hydride in THF (1 M, 3.23 mL, 3 mmol). The reaction was stirred at 65 °C overnight, and then, it was cooled down to 0 °C. A few drops of an aqueous solution of 5% NaOH were added, and the mixture was allowed to reach rt and stirred overnight. The resulting suspension was filtered and washed with ethyl acetate. The combined filtrates were washed with water, and the combined organic layers were dried over Na_2SO_4, filtered, and concentrated to dryness to give 7-(2-(4-benzylpiperazin-1-yl)ethyl)aniline (**13-2**) as a dark oil (0.381 g, 79% yield). ^{1}H NMR (400 MHz, CD_3OD): δ 7.47−7.19 (m, 5H), 7.18−7.03 (m, 2H), 6.79−6.54 (m, 3H), 3.55 (s, 2H), 3.22 (dd, J = 6.2, 7.2 Hz, 2H), 2.61 (dd, J = 6.3, 7.1 Hz, 2H), 2.68−2.39 (m, 8H). HPLC-MS: m/z = 296 $[M + H]^+$.

*N-(2-(4-Benzylpiperazin-1-yl)-2-methylpropyl)aniline (**13-3**). Step 1.* TEA (1.4 mL, 10 mmol) and ethyl 2-bromo-2-methylpropanoate (1.5 mL, 10 mmol) were added to a solution of 1-benzylpiperazine (**9-1**, 0.6 g, 3.4 mmol) in EtOH (15 mL) in a microwave vial under a nitrogen atmosphere. The reaction mixture was heated under microwave irradiation for 3.5 h at 150 °C, after which it was allowed to reach rt. The solvent was concentrated in vacuo, and the residue was dissolved in DCM and washed twice with water. The aqueous phase was acidified to pH 2 and extracted twice with DCM. The organic layers were combined, dried over Na_2SO_4, filtered, and concentrated to give ethyl 2-(4-benzylpiperazin-1-yl)-2-methylpropanoate (656 mg, 66% yield) as a crude ester that was submitted to hydrolysis without further purification. HPLC-MS: m/z = 291 $[M + H]^+$. Aqueous NaOH (1 M, 4.2 mL, 40 mmol) was added to a solution of the previous compound (648 mg, 2.23 mmol) in MeOH (20 mL). The mixture was refluxed for 6 h and then concentrated under vacuum to afford 2-(4-benzylpiperazin-1-yl)-2-methylpropanoic acid (**24**), which was used in the following step without further purification. HPLC-MS: m/z = 263 $[M + H]^+$.

Step 2. A mixture of compound **24** (0.6 g, 2.28 mmol) and HOBt (0.7 g, 4.57 mmol) was added to a solution of 1-ethyl-3-(3-dimethylaminopropyl)carbodiimide (EDC) (0.87 g, 4.57 mmol) in DMF (3 mL). Then, aniline (**22**, 311 μL, 3.43 mmol) and TEA (495 μL, 3.55 mmol) were added, and the reaction mixture was stirred at rt overnight. The mixture was partitioned between water and ethyl acetate/ethyl ether (1:1), and the organic layer was washed twice with an aqueous basic solution, twice with an aqueous acid solution, and twice with water. Finally, the organic layer was dried over Na_2SO_4, filtered, and concentrated to give 2-(4-benzylpiperazin-1-yl)-2-methyl-*N*-phenylpropanamide (174.5 mg, 22% yield). HPLC-MS: m/z = 338 $[M + H]^+$. The alane solution was then prepared for reduction of this carboxamide compound: to a vigorously stirred solution of $LiAlH_4$ (1 M in THF, 15 mmol) at −70 °C, sulfuric acid (0.3 mL) was added dropwise. The reaction was stirred with the temperature increasing from −70 °C to −50 °C for 2 h and left at rt for 2 h without stirring (a white solid appeared). In a round-bottomed flask, the previously prepared fresh alane solution (1.07 mL, 3 eq) decanted *via* a syringe was cooled to 0 °C under an argon atmosphere. 2-(4-Benzylpiperazin-1-yl)-2-methyl-*N*-phenylpropanamide (120 mg, 0.36 mmol) dissolved in THF (5 mL) was added dropwise, and the mixture was stirred at 0 °C for 1.5 h. The reaction was quenched with ethyl acetate and ice water. The aqueous layer was extracted several times with ethyl acetate. The combined organic layers were washed with water, dried over Na_2SO_4, filtered, and concentrated to dryness. The residue was purified by flash chromatography on silica gel, gradient DCM to MeOH/DCM (90:10), to give *N*-(2-(4-benzylpiperazin-1-yl)-2-methylpropyl)aniline (**13-3**) (32.5 mg, 28% yield). ^{1}H NMR (400 MHz, CD_3OD): δ 7.38−7.30 (m, 4H), 7.30−7.22 (m, 1H), 7.14−7.06 (m, 2H), 6.64−6.57 (m, 3H), 3.53 (s, 2H), 2.98 (s, 2H), 2.74−2.57 (m, 4H), 2.57−2.43 (m, 4H), 1.13 (s, 6H). HPLC-MS: purity 94%, m/z = 324 $[M + H]^+$.

*N-((1-(4-Benzylpiperazin-1-yl)cyclopropyl)methyl)-6-(trifluoromethyl)pyridin-2-amine (**13-4a**). Step 1.* Thionyl chloride (19.75 mL, 266 mmol) in anhydrous DCM (40 mL) was added to a 0 °C cooled solution of 2,2′-(benzylazanediyl)diethanol (**25**, 17.29 g, 89 mmol) in DCM (15 mL), and the reaction mixture was stirred at rt

https://doi.org/10.1021/acs.jmedchem.1c00417
J. Med. Chem. 2021, 64, 10139−10154

overnight. The solvent was removed to dryness to give *N*-benzyl-2-chloro-*N*-(2-chloroethyl)ethanamine hydrochloride (**26**, 23.78 g, 100% crude yield), which was used in the next step without further purification. ^{1}H NMR (400 MHz, $CDCl_3$): δ 7.76−7.63 (m, 2H), 7.57−7.42 (m, 3H), 4.38 (s, 2H), 4.06 (t, J = 6.8 Hz, 4H), 3.47 (t, J = 6.8 Hz, 4H). HPLC-MS: m/z = 232 $[M + H]^+$.

Step 2. Compound **26** (10.37 g, 38.61 mmol) was added to a solution of ethyl 1-aminocyclopropanecarboxylate hydrochloride (6.4 g, 38.6 mmol) and $NaHCO_3$ (17.5 g, 208.5 mmol) in EtOH (200 mL). The reaction mixture was stirred at 80 °C for 4 h and overnight at rt. The solvent was concentrated, and the crude product was diluted with ethyl acetate and water. The layers were separated, and the organic layer was dried over Na_2SO_4, filtered, and concentrated. The crude residue was purified by flash chromatography on silica gel and eluents CH/ethyl acetate (100:0 to 0:100) to give ethyl 1-(4-benzylpiperazin-1-yl)cyclopropanecarboxylate (2.86 g, 24% yield). HPLC-MS: m/z = 289 $[M + H]^+$. The previous compound (2.36 g, 8.21 mmol) was dissolved in EtOH (100 mL), and KOH (5.4 g, 82.07 mmol) in EtOH (50 mL) was added. The solution was heated at 120 °C for 5 h. The reaction mixture was cooled at 0 °C, and acetic acid (4.7 mL, 82.07 mmol) was added. After stirring for 10 min, the mixture was concentrated under vacuum. The residue was treated with ethyl acetate, and the solid thus obtained was filtered and washed several times with water. Then, it was dried in vacuo to afford 1-(4-benzylpiperazin-1-yl)cyclopropanecarboxylic acid (**27**) as a beige solid (1.76 g, 82% yield). ^{1}H NMR (400 MHz, CD_3OD): δ 7.60−7.37 (m, 5H), 4.19 (s, 2H), 3.37−3.17 (m, 4H), 3.13−2.94 (m, 4H), 1.27 (q, J = 3.8 Hz, 2H), 0.95 (q, J = 3.7 Hz, 2H). HPLC-MS: purity 100%, m/z = 261 $[M + H]^+$.

Step 3. *N*-[(Dimethylamino)-1*H*-1,2,3-triazolo-[4,5-*b*]pyridin-1-ylmethylene]-*N*-methylmethanaminium hexafluorophosphate *N*-oxide (HATU, 6.3 g, 17 mmol), TEA (4.2 mL, 30 mmol), and ammonium bicarbonate (1.19 g, 15 mmol) were added to a solution of **27** (12.7 g, 15.07 mmol) in DMF (100 mL) at 0 °C, and the mixture was stirred at rt for 2 days. The reaction mixture was partitioned between water and ethyl acetate/Et_2O (1/1), and the combined organic layers were washed twice with water, dried over $MgSO_4$, filtered, and concentrated to afford 1-(4-benzylpiperazin-1-yl)cyclopropanecarboxamide (1.75 g, 45% yield). HPLC-MS: m/z = 260 $[M + H]^+$. A solution of $LiAlH_4$ (1 M in THF, 13.5 mL, 13.5 mmol) was added to a −10 °C cooled solution of the previous compound (1.75 g, 6.76 mmol) in dry THF (20 mL). The reaction mixture was stirred at this temperature for 5 h, allowed to reach rt, and stirred overnight. The suspension thus obtained was cooled down to 0 °C, and diluted aqueous NaOH was added. The mixture was filtered and rinsed with ethyl acetate. The filtrate was washed with H_2O, and the combined organic layers were dried over Na_2SO_4, filtered, and concentrated to give (1-(4-benzylpiperazin-1-yl)-cyclopropyl)methanamine as an oil (0.9 g, 54% yield). HPLC-MS: m/z = 246 $[M + H]^+$. A portion of this compound (665 mg, 2.7 mmol), 2-bromo-6-(trifluoromethyl)pyridine (**12-1**, 735 mg, 3.26 mmol), $Pd_2(dba)_3$ (101.2 mg, 0.163 mmol), BINAP (124 mg, 0.136 mmol), and ^{t}BuOK (395 mg, 3.52 mmol) were added to a Schlenk tube, that was evacuated and backfilled with argon (three cycles). Then, anydrous THF (15 mL) was added, and the reaction mixture was stirred at 50 °C overnight. The solvents were evaporated, and the residue was dissolved in ethyl acetate and aqueous saturated $NaHCO_3$ solution. The aqueous layer was extracted with ethyl acetate, and the combined organic layers were dried over Na_2SO_4, filtered, and concentrated. The crude product was purified by flash chromatography on silica gel, gradient CH/ethyl acetate from (100:0) to (0:100), to give *N*-((1-(4-benzylpiperazin-1-yl)cyclopropyl)methyl)-6-(trifluoromethyl)pyridin-2-amine (**13-4a**) as a solid (628 mg, 53% yield). ^{1}H NMR (400 MHz, CD_3OD): δ 7.48 (ddq, J = 0.7, 7.3, 8.7 Hz, 1H), 7.33−7.20 (m, 5H), 6.82 (dd, J = 0.7, 7.2 Hz, 1H), 6.64 (dq, J = 0.7, 8.6 Hz, 1H), 3.54 (s, 2H), 3.48 (s, 2H), 2.84 (t, J = 4.9 Hz, 4H), 2.50−2.32 (m, 4H), 0.68−0.62 (m, 2H), 0.62−0.54 (m, 2H). HPLC-MS: purity 95%, m/z = 391 $[M + H]^+$.

*N-((4-(1-Benzylpiperidin-4-yl)tetrahydro-2H-pyran-4-yl)methyl)-N-(6-(trifluoromethyl)pyridin-2-yl)propionamide (**36**). Step 1.* To a solution of tetrahydro-2*H*-pyran-4-carbonitrile (**28**, 4.85 g, 43.6 mmol) in dry THF (41 mL), cooled at −78 °C, LDA solution (30.5 mL, 1.5 M in a mixture of THF/ethylbenzene/heptane, 45.8 mmol) was added dropwise under a nitrogen atmosphere. The mixture was stirred at −50 °C for 45 min, and then, it was cooled at −78 °C. A solution of *tert*-butyl 4-oxopiperidine-1-carboxylate (**29**, 8.69 g, 43.6 mmol) in dry THF (5.2 mL) was added, and the reaction mixture was stirred at −78 °C for 2 h. Then, NH_4Cl saturated aqueous solution was added, and the mixture was extracted with ethyl acetate. The organic phases were combined, dried over $MgSO_4$, filtered, and concentrated to dryness. The residue was purified by flash chromatography on silica gel, gradient DCM to MeOH/DCM (10:90), to give *tert*-butyl 4-(4-cyanotetrahydro-2*H*-pyran-4-yl)-4-hydroxypiperidine-1-carboxylate (**30**, 7.11 g, 53% yield). ^{1}H NMR (400 MHz, $CDCl_3$): δ 4.21−3.95 (m, 4H), 3.72 (td, J = 2.5, 12.0 Hz, 2H), 3.03 (t, J = 12.3 Hz, 2H), 1.91−1.71 (m, 6H), 1.71−1.60 (m, 2H), 1.46 (s, 9H). HPLC-MS: m/z = 255 $[M + H - 56]^+$ (−*t*Bu, Boc fragmentation).

Step 2. To a solution of compound **30** (6.10 g, 19.7 mmol) in toluene (71 mL), (methoxycarbonylsulfamoyl)triethylammonium hydroxide inner salt ("Burgess reagent", 7.03 g, 29.5 mmol) was added, and the mixture was heated at 90 °C overnight under a nitrogen atmosphere. It was then cooled to rt, and water and DCM were added. The aqueous phase was back-extracted with DCM. The organic phases were combined, washed with saturated $NaHCO_3$ solution, dried over Na_2SO_4, filtered, and concentrated to dryness to give *tert*-butyl 4-(4-cyanotetrahydro-2*H*-pyran-4-yl)-5,6-dihydropyridine-1(2*H*)-carboxylate (**31**, 6.14 g crude product, 5.75 g theoretical weight; quantitative yield). ^{1}H NMR (400 MHz, $CDCl_3$): δ 5.78 (br s, 1H), 4.06−3.94 (m, 4H), 3.84−3.73 (m, 2H), 3.54 (t, J = 5.6 Hz, 2H), 2.27−2.18 (m, 2H), 1.90−1.77 (m, 4H), 1.48 (s, 9H). HPLC-MS: m/z = 237 $[M + H - 56]^+$ (−*t*Bu, Boc fragmentation).

Step 3. A mixture of compound **31** (6.14 g crude, 19.7 mmol) and palladium (1.23 g, 5% wt on charcoal, wet) in EtOH (115 mL) was stirred at rt under 1 bar of H_2 overnight. Then, the solids were filtered off over a pad of Celite, and the solvent was evaporated to dryness. The residue was purified by flash chromatography, silica gel, gradient DCM to MeOH/DCM (10:90), to give *tert*-butyl 4-(4-cyanotetrahydro-2*H*-pyran-4-yl)piperidine-1-carboxylate (**32**, 4.04 g, 70% yield). ^{1}H NMR (400 MHz, $CDCl_3$): δ 4.38−4.12 (m, 2H), 4.05−3.93 (m, 2H), 3.71 (td, J = 1.9, 12.4 Hz, 2H), 2.65 (t, J = 11.4 Hz, 2H), 1.88 (dd, J = 2.0, 13.5 Hz, 2H), 1.80 (d, J = 10.9 Hz, 2H), 1.60 (ddd, J = 4.5, 10.0, 17.0 Hz, 2H), 1.46 (s, 9H), 1.50−1.34 (m, 3H). HPLC-MS: purity 91%, m/z = 239.1 $[M + H - 56]^+$ (−*t*Bu, Boc fragmentation).

Step 4. To a solution of compound **32** (4.0 g, 13.6 mmol) in DCM (40 mL), TFA (10.4 mL, 136 mmol) was added, and the reaction mixture was stirred at rt for 1 h. The solvent was evaporated to dryness to give 4-(piperidin-4-yl)tetrahydro-2*H*-pyran-4-carbonitrile trifluoroacetate (7.18 g, 4.19 g theoretical weight, quantitative yield). This crude compound and benzaldehyde (1.3 mL, 17.7 mmol) were dissolved in dry THF (92 mL), and AcOH (1.73 mL, 30.2 mmol) was added. The mixture was stirred at rt for 15 min, and then, sodium triacetoxyborohydride (7.99 g, 40.8 mmol) was added in portions. The resulting mixture was stirred at rt overnight. Then, concentrated NH_4OH (50 mL) was carefully added, and it was extracted with ethyl acetate. The organic phases were combined, washed with brine, dried over $MgSO_4$, filtered, and concentrated to dryness. The residue was purified by flash chromatography, silica gel, gradient DCM to MeOH/DCM (25:75), to give 4-(1-benzylpiperidin-4-yl)tetrahydro-2*H*-pyran-4-carbonitrile (**33**, 1.75 g, 45% yield). ^{1}H NMR (400 MHz, $CDCl_3$): δ 7.34−7.29 (m, 4H), 7.28−7.22 (m, 1H), 3.97 (ddt, J = 1.0, 4.6, 12.3 Hz, 2H), 3.71 (td, J = 1.9, 12.3 Hz, 2H), 3.50 (s, 2H), 3.06−2.93 (m, 2H), 1.93 (td, J = 2.4, 11.9 Hz, 2H), 1.86 (dq, J = 2.5, 13.5 Hz, 2H), 1.81−1.72 (m, 2H), 1.65−1.50 (m, 4H), 1.31 (tt, J = 3.7, 12.1 Hz, 1H). HPLC-MS purity 98%; m/z 285 $[M + H]^+$.

Step 5. Following a similar procedure to the one described in step 2 of the synthesis of compound **15r**, (4-(1-benzylpiperidin-4-yl)-tetrahydro-2*H*-pyran-4-yl)methanamine (**34**) was obtained (879 mg, 50% yield). ^{1}H NMR (400 MHz, $CDCl_3$): δ 7.33−7.28 (m, 4H),

https://doi.org/10.1021/acs.jmedchem.1c00417
J. Med. Chem. 2021, 64, 10139−10154

7.27−7.21 (m, 1H), 3.72 (dt, J = 4.3, 11.8 Hz, 2H), 3.59 (ddd, J = 2.8, 10.3, 11.8 Hz, 2H), 3.49 (s, 2H), 2.98 (ddd, J = 1.7, 3.4, 12.4 Hz, 2H), 2.82 (s, 2H), 1.96−1.84 (m, 2H), 1.66−1.56 (m, 4H), 1.46−1.31 (m, 5H). HPLC-MS: purity 100%; m/z = 289 $[M + H]^+$.

Step 6. Following a similar procedure to the one described in step 3 of the synthesis of compound **15r**, *N*-((4-(1-benzylpiperidin-4-yl)tetrahydro-2*H*-pyran-4-yl)methyl)-6-(trifluoromethyl)pyridin-2-amine (**35**) was obtained (712 mg, 54% yield). ^{1}H NMR (400 MHz, $CDCl_3$): δ 7.48 (t, J = 7.9 Hz, 1H), 7.36−7.29 (m, 5H), 6.89 (d, J = 7.3 Hz, 1H), 6.53 (d, J = 8.5 Hz, 1H), 4.63 (br s, 1H), 3.75−3.69 (m, 4H), 3.65−3.52 (m, 2H), 3.50 (s, 2H), 3.06−2.93 (m, 2H), 1.93 (t, J =11.9 Hz, 2H), 1.80−1.58 (m, 4H), 1.55−1.45 (m, 1H), 1.44−1.30 (m, 2H). HPLC-MS: purity 96%, m/z = 434 $[M + H]^+$.

Step 7. Following a similar procedure to the one described in step 4 of the synthesis of compound **15r**, *N*-((4-(1-benzylpiperidin-4-yl)tetrahydro-2*H*-pyran-4-yl)methyl)-6-(trifluoromethyl)pyridin-2-amine (**36**) was obtained (49 mg, 33% yield). ^{1}H NMR (400 MHz, CD_3OD): δ 8.17 (t, J = 7.9 Hz, 1H), 7.82 (d, J = 8.0 Hz, 2H), 7.81 (d, J = 7.7 Hz, 1H), 7.59−7.46 (m, 5H), 4.28 (s, 2H), 4.21 (s, 2H), 3.63−3.47 (m, 4H), 3.46−3.36 (m, 2H), 3.06−2.77 (m, 2H), 2.22 (q, J = 7.3 Hz, 2H), 2.03 (d, J = 13.9 Hz, 2H), 1.83 (t, J = 12.3 Hz, 1H), 1.64 (t, J = 13.0 Hz, 2H), 1.50 (ddd, J = 4.2, 9.1, 13.6 Hz, 2H), 1.26 (d, J = 14.4 Hz, 2H), 1.04 (t, J = 7.4 Hz, 3H). HPLC-MS: purity 94%, m/z = 490 $[M + H]^+$.

In Vitro Studies. Human radioligand assays of the σ_1R and MOR and human MOR functionality and hERG assays were carried out under the experimental conditions previously described.[24]

In Vitro Metabolic Stability and PK Studies. Experimental details of *in vitro* metabolic stability in human and mice liver microsomes and PKs in rodents are provided in the Supporting Information.

In Vivo Efficacy Studies. The experimental details of the paw pressure test, PSNL, and intestinal transit inhibition models are given in the Supporting Information. All animal husbandry and experimental procedures complied with the European guidelines regarding the protection of animals used for experimental and other scientific purposes international standards (European Communities Council directive 2010/63) and were approved by the local ethics committee.

■ ASSOCIATED CONTENT

Supporting Information

The Supporting Information is available free of charge at https://pubs.acs.org/doi/10.1021/acs.jmedchem.1c00417.

Molecular formula strings (CSV)

Analytical data for all the final compounds and intermediates, HPLC traces for final compounds, calculated log $D_{7.4}$ values of final compounds, experimental details of *in vitro* metabolic stability and PK studies, and experimental details of *in vivo* efficacy studies (PDF)

■ AUTHOR INFORMATION

Corresponding Author

Mónica García − *ESTEVE Pharmaceuticals, Barcelona 08038, Spain;* Present Address: WELAB Barcelona, Parc Científic de Barcelona, C/ Baldiri Reixac 4-8, 08028 Barcelona, Spain; orcid.org/0000-0003-2338-8338; Email: mgarcial@welab.barcelona

Authors

Virginia Llorente − *ESTEVE Pharmaceuticals, Barcelona 08038, Spain;* Present Address: WELAB Barcelona, Parc Científic de Barcelona, C/ Baldiri Reixac 4-8, 08028 Barcelona, Spain

Lourdes Garriga − *ESTEVE Pharmaceuticals, Barcelona 08038, Spain;* Present Address: WELAB Barcelona, Parc Científic de Barcelona, C/ Baldiri Reixac 4-8, 08028 Barcelona, Spain

Ute Christmann − *ESTEVE Pharmaceuticals, Barcelona 08038, Spain;* Present Address: WELAB Barcelona, Parc Científic de Barcelona, C/ Baldiri Reixac 4-8, 08028 Barcelona, Spain

Sergi Rodríguez-Escrich − *ESTEVE Pharmaceuticals, Barcelona 08038, Spain;* Present Address: WELAB Barcelona, Parc Científic de Barcelona, C/ Baldiri Reixac 4-8, 08028 Barcelona, Spain

Marina Virgili − *Enantia, S.L., Barcelona 08028, Spain*

Begoña Fernández − *ESTEVE Pharmaceuticals, Barcelona 08038, Spain;* Present Address: WELAB Barcelona, Parc Científic de Barcelona, C/ Baldiri Reixac 4-8, 08028 Barcelona, Spain

Magda Bordas − *ESTEVE Pharmaceuticals, Barcelona 08038, Spain;* Present Address: WELAB Barcelona, Parc Científic de Barcelona, C/ Baldiri Reixac 4-8, 08028 Barcelona, Spain

Eva Ayet − *ESTEVE Pharmaceuticals, Barcelona 08038, Spain;* Present Address: WELAB Barcelona, Parc Científic de Barcelona, C/ Baldiri Reixac 4-8, 08028 Barcelona, Spain

Javier Burgueño − *ESTEVE Pharmaceuticals, Barcelona 08038, Spain;* Present Address: WELAB Barcelona, Parc Científic de Barcelona, C/ Baldiri Reixac 4-8, 08028 Barcelona, Spain

Marta Pujol − *ESTEVE Pharmaceuticals, Barcelona 08038, Spain;* Present Address: WELAB Barcelona, Parc Científic de Barcelona, C/ Baldiri Reixac 4-8, 08028 Barcelona, Spain

Albert Dordal − *ESTEVE Pharmaceuticals, Barcelona 08038, Spain;* Present Address: WELAB Barcelona, Parc Científic de Barcelona, C/ Baldiri Reixac 4-8, 08028 Barcelona, Spain

Enrique Portillo-Salido − *ESTEVE Pharmaceuticals, Barcelona 08038, Spain;* Present Address: WELAB Barcelona, Parc Científic de Barcelona, C/ Baldiri Reixac 4-8, 08028 Barcelona, Spain

Georgia Gris − *ESTEVE Pharmaceuticals, Barcelona 08038, Spain;* Present Address: WELAB Barcelona, Parc Científic de Barcelona, C/ Baldiri Reixac 4-8, 08028 Barcelona, Spain

José Miguel Vela − *ESTEVE Pharmaceuticals, Barcelona 08038, Spain;* Present Address: WELAB Barcelona, Parc Científic de Barcelona, C/ Baldiri Reixac 4-8, 08028 Barcelona, Spain

Carmen Almansa − *ESTEVE Pharmaceuticals, Barcelona 08038, Spain;* Present Address: WELAB Barcelona, Parc Científic de Barcelona, C/ Baldiri Reixac 4-8, 08028 Barcelona, Spain; orcid.org/0000-0001-5665-4685

Complete contact information is available at: https://pubs.acs.org/10.1021/acs.jmedchem.1c00417

Notes

The authors declare no competing financial interest.

■ ACKNOWLEDGMENTS

We thank Sandra Silvestre, Mª Paz Diez, and Joana Berrocal for their expert technical contribution to the compound syntheses; Adriana Port, Raquel Enrech, Joan Andreu Morató, Mónica Carro, Edmundo Ortega, Manel Merlos, Inés Álvarez, Pilar

Pérez, Xavier Monroy, Xavier Farré, Enric Hernández, Raquel Fernández-Reinoso, Sandra Yeste, Maite Serafini, Mª José Pretel, Alba Vidal, Carmen Segalés, Bertrand Aubel, Alicia Pardo, Ana Paz Marín, Antonio Rodriguez Fernández de Henestrosa, and Daniel Zamanillo for their expert contribution to analytical, *in vitro* and *in vivo* studies; and Carlos Pérez and Eduardo Villarroel for their contribution to compound management. This work was a part of activities in R&D Projects IDI20130943 and IDI20150915 supported by the Spanish Ministerio de Economía y Competitividad (MINECO) through the Centro para el Desarrollo Tecnológico Industrial (CDTI), co-financed by the European Union through the European Regional Development Fund (ERDF; Fondo Europeo de Desarrollo Regional, FEDER).

■ ABBREVIATIONS

ADME, absorption, distribution, metabolism, and excretion; BCS, biopharmaceutics classification system; CNS, central nervous system; ESI, electrospray ionization; hERG, human ether-a-go-go-related gene; HPLC, high-performance liquid chromatography; HTS, high-throughput screening; MOR, μ-opioid receptor; MS, mass spectrometry; MW, microwave; PDA, photodiode array; QTOF, quadrupole time-of-flight; SAR, structure−activity relationships; σ_1R, sigma-1 receptor; TEA, triethylamine

■ REFERENCES

(1) Gureje, O.; Von Korff, M.; Simon, G. E.; Gater, R. Persistent Pain and Well-being. *JAMA* **1998**, *280*, 147−151.
(2) Lerman, S. F.; Rudich, Z.; Brill, S.; Shalev, H.; Shahar, G. Longitudinal associations between depression, anxiety, pain, and pain-related disability in chronic pain patients. *Psychosom. Med.* **2015**, *77*, 333−341.
(3) Goldberg, D. S.; McGee, S. J. Pain as a global public health priority. *BMC Public Health* **2011**, *11*, 770.
(4) Galanter, M.; Kleber, H. D.; Brady, K. T. *The American Psychiatric Publishing Textbook of Substance Abuse Treatment*; American Psychiatric Publishing: Washington CD, 2014.
(5) Dickenson, A. H.; Suzuki, R. Opioids in neuropathic pain: Clues from animal studies. *Eur. J. Pain* **2005**, *9*, 113−116.
(6) Ballantyne, J. C.; Shin, N. S. Efficacy of Opioids for Chronic Pain. *Clin. J. Pain* **2008**, *24*, 469−478.
(7) Opioids and Pain Relief: A Historical Perspective. *Progress in Pain Research and Management*; Meldrum, M. L., Ed.; IASP Press: Seattle, 2003; Vol 25.
(8) Jones, M. R.; Viswanath, O.; Peck, J.; Kaye, A. D.; Gill, J. S.; Simopoulos, T. T. A brief history of the opioid epidemic and strategies for pain medicine. *Pain Ther.* **2018**, *7*, 13−21.
(9) Pang, M.-H.; Kim, Y.; Jung, K. W.; Cho, S.; Lee, D. H. A series of case studies: practical methodology for identifying antinociceptive multi-target drugs. *Drug Discovery Today* **2012**, *17*, 425−434.
(10) Morphy, R.; Rankovic, Z. Designed multiple ligands. An emerging drug discovery paradigm. *J. Med. Chem.* **2005**, *48*, 6523−6543.
(11) Chien, C. C.; Pasternak, G. W. Sigma antagonists potentiate opioid analgesia in rats. *Neurosci. Lett.* **1995**, *190*, 137−139.
(12) Kim, F. J.; Kovalyshyn, I.; Burgman, M.; Neilan, C.; Chien, C.-C.; Pasternak, G. W. σ1 Receptor Modulation of G-Protein-Coupled Receptor Signaling: Potentiation of Opioid Transduction Independent from Receptor Binding. *Mol. Pharmacol.* **2010**, *77*, 695−703.
(13) Mei, J.; Pasternak, G. W. ς1 Receptor Modulation of Opioid Analgesia in the Mouse. *J. Pharmacol. Exp. Ther.* **2002**, *300*, 1070−1074.
(14) Pan, Y. X.; Mei, J.; Xu, J.; Wan, B. L.; Zuckerman, A.; Pasternak, G. W. Cloning and characterization of a mouse sigma1 receptor. *J. Neurochem.* **1998**, *70*, 2279−2285.
(15) Martínez-Navarro, M.; Maldonado, R.; Baños, J.-E. Why mu-opioid agonists have less analgesic efficacy in neuropathic pain? *Eur. J. Pain* **2019**, *23*, 435−454.
(16) de la Puente, B.; Nadal, X.; Portillo-Salido, E.; Sánchez-Arroyos, R.; Ovalle, S.; Palacios, G.; Muro, A.; Romero, L.; Entrena, J. M.; Baeyens, J. M.; López-García, J. A.; Maldonado, R.; Zamanillo, D.; Vela, J. M. Sigma-1 receptors regulate activity-induced spinal sensitization and neuropathic pain after peripheral nerve injury. *Pain* **2009**, *145*, 294−303.
(17) Zamanillo, D.; Romero, L.; Merlos, M.; Vela, J. M. Sigma 1 receptor: A new therapeutic target for pain. *Eur. J. Pharmacol.* **2013**, *716*, 78−93.
(18) Cendán, C. M.; Pujalte, J. M.; Portillo-Salido, E.; Montoliu, L.; Baeyens, J. M. Formalin-induced pain is reduced in σ1 receptor knockout mice. *Eur. J. Pharmacol.* **2005**, *511*, 73−74.
(19) Díaz, J. L.; Cuberes, R.; Berrocal, J.; Contijoch, M.; Christmann, U.; Fernández, A.; Port, A.; Holenz, J.; Buschmann, H.; Laggner, C.; Serafini, M. T.; Burgueño, J.; Zamanillo, D.; Merlos, M.; Vela, J. M.; Almansa, C. Synthesis and Biological Evaluation of the 1-Arylpyrazole Class of σ1 Receptor Antagonists: Identification of 4-{2-[5-Methyl-1-(naphthalen-2-yl)-1H-pyrazol-3-yloxy]ethyl}-morpholine (S1RA, E-52862). *J. Med. Chem.* **2012**, *55*, 8211−8224.
(20) Gris, G.; Portillo-Salido, E.; Aubel, B.; Darbaky, Y.; Deseure, K.; Vela, J. M.; Merlos, M.; Zamanillo, D. The selective sigma-1 receptor antagonist E-52862 attenuates neuropathic pain of different aetiology in rats. *Sci. Rep.* **2016**, *6*, 24591.
(21) Vidal-Torres, A.; de la Puente, B.; Rocasalbas, M.; Touriño, C.; Andreea Bura, S.; Fernández-Pastor, B.; Romero, L.; Codony, X.; Zamanillo, D.; Buschmann, H.; Merlos, M.; Manuel Baeyens, J.; Maldonado, R.; Vela, J. M. Sigma-1 receptor antagonism as opioid adjuvant strategy: Enhancement of opioid antinociception without increasing adverse effects. *Eur. J. Pharmacol.* **2013**, *711*, 63−72.
(22) E. U. Clinical Trials Register. An exploratory, randomized, double blind, placebo controlled, parallel groups Phase II clinical trial to evaluate the efficacy and safety of E-52862 (400 mg) by oral route, as part of an analgesic therapy balanced with morphine, followed by an open label extension, in the treatment of post-operative pain due to abdominal hysterectomy [Internet]. www.clinicaltrialsregister.eu/ctr-search/trial/2011-003302-24/results (accessed Jun 03, 2020).
(23) García, M.; Virgili, M.; Alonso, M.; Alegret, C.; Fernández, B.; Port, A.; Pascual, R.; Monroy, X.; Vidal-Torres, A.; Serafini, M.-T.; Vela, J. M.; Almansa, C. 4-Aryl-1-oxa-4,9-diazaspiro[5.5]undecane Derivatives as Dual μ-Opioid Receptor Agonists and σ1 Receptor Antagonists for the Treatment of Pain. *J. Med. Chem.* **2020**, *63*, 2434−2454.
(24) García, M.; Virgili, M.; Alonso, M.; Alegret, C.; Farran, J.; Fernández, B.; Bordas, M.; Pascual, R.; Burgueño, J.; Vidal-Torres, A.; Fernández de Henestrosa, A. R.; Ayet, E.; Merlos, M.; Vela, J. M.; Plata-Salamán, C. R.; Almansa, C. Discovery of EST73502, a Dual μ-Opioid Receptor Agonist and σ1 Receptor Antagonist Clinical Candidate for the Treatment of Pain. *J. Med. Chem.* **2020**, *63*, 15508−15526.
(25) *An Exploratory, Randomised, Double-Blind, Placebo and Active Therapy Controlled, Phase I Study, to Assess the Safety, Tolerability, Pharmacokinetics, Pharmacodynamics, and Food- Effect of Single and Multiple Ascending Oral Doses of EST73502 in Healthy Adults and Patients with Chronic, Moderate Moderate-To To-Severe Osteoarthritis Pain. (Study EudraCT Number 2018-000258-23)*, 2018.
(26) García, M.; Almansa, C.; Llorente, A. V.; Garriga, L.; Christmann, U. Preparation of Substituted Amide Derivatives Having Multimodal Activity against Pain. WO 2017016669, 2017.
(27) Zhang, C.; Tan, C.; Zu, X.; Zhai, X.; Liu, F.; Chu, B.; Ma, X.; Chen, Y.; Gong, P.; Jiang, Y. Exploration of (*S*)-3-aminopyrrolidine as a potentially interesting scaffold for discovery of novel Abl and PI3K dual inhibitors. *Eur. J. Med. Chem.* **2011**, *46*, 1404−1414.
(28) Baeza, A.; Nájera, C.; Sansano, J. M. Solvent-free synthesis of racemic α-aminonitriles. *Synthesis* **2007**, *8*, 1230−1234.
(29) DeHaven-Hudkins, D. L.; Fleissner, L. C.; Ford-Rice, F. Y. Characterization of the binding of [3H](+)-pentazocine to σ

https://doi.org/10.1021/acs.jmedchem.1c00417
J. Med. Chem. 2021, 64, 10139−10154

recognition sites in guinea pig brain. *Eur. J. Pharmacol.* **1992**, *227*, 371−378.
(30) Thum, S.; Schepmann, D.; Ayet, E.; Pujol, M.; Nieto, F. R.; Ametamey, S. M.; Wünsch, B. Tetrahydro-3-benzazepines with fluorinated side chains as NMDA and σ1 receptor antagonists: Synthesis, receptor affinity, selectivity and antiallodynic activity. *Eur. J. Med. Chem.* **2019**, *177*, 47−62.
(31) Burgueño, J.; Pujol, M.; Monroy, X.; Roche, D.; Varela, M. J.; Merlos, M.; Giraldo, J. A complementary scale of biased agonism for agonists with differing maximal responses. *Sci. Rep.* **2017**, *7*, 15389.
(32) Morphy, R.; Rankovic, Z. The physicochemical challenges of designing multiple ligands. *J. Med. Chem.* **2006**, *49*, 4961−4970.
(33) (a) Obach, R. S.; Baxter, J. G.; Liston, T. E.; Silber, B. M.; Jones, B. C.; MacIntyre, F.; Rance, D. J.; Wastall, P. The prediction of human pharmacokinetic parameters from preclinical and in vitro metabolism data. *J. Pharmacol. Exp. Ther.* **1997**, *283*, 46−58. (b) Obach, R. S. Prediction of human clearance of twenty-nine drugs from hepatic microsomal intrinsic clearance data: an examination of in vitro half-life approach and nonspecific binding to microsomes. *Drug Metab. Dispos.* **1999**, *27*, 1350−1359.
(34) Diaz, G. J.; Daniell, K.; Leitza, S. T.; Martin, R. L.; Su, Z.; McDermott, J. S.; Cox, B. F.; Gintant, G. A. The [^{3}H]-dofetilide binding assay is a predictive screening tool for hERG blockade and proarrhythmia: Comparison of intact cell and membrane preparations and effects of altering $[K^+]_o$. *J. Pharmacol. Toxicol. Methods* **2004**, *50*, 187−199.
(35) Pascual, R.; Almansa, C.; Plata-Salamán, C.; Vela, J. M. A new pharmacophore model for the design of sigma-1 ligands validated on a large experimental dataset. *Front. Pharmacol.* **2019**, *10*, 519.
(36) Laggner, C.; Schieferer, C.; Fiechtner, B.; Poles, G.; Hoffmann, R. D.; Glossmann, H.; Langer, T.; Moebius, F. F. Discovery of High-Affinity Ligands of σ1Receptor, ERG2, and Emopamil Binding Protein by Pharmacophore Modeling and Virtual Screening. *J. Med. Chem.* **2005**, *48*, 4754−4764.
(37) Stepan, A. F.; Karki, K.; McDonald, W. S.; Dorff, P. H.; Dutra, J. K.; DiRico, K. J.; Won, A.; Subramanyam, C.; Efremov, I. V.; O'Donnell, C. J.; Nolan, C. E.; Becker, S. L.; Pustilnik, L. R.; Sneed, B.; Sun, H.; Lu, Y.; Robshaw, A. E.; Riddell, D.; O'Sullivan, T. J.; Sibley, E.; Capetta, S.; Atchison, K.; Hallgren, A. J.; Miller, E.; Wood, A.; Obach, R. S. Metabolism-Directed Design of Oxetane-Containing Arylsulfonamide Derivatives as γ-Secretase Inhibitors. *J. Med. Chem.* **2011**, *54*, 7772−7783.
(38) Wessjohann, L. A.; Brandt, W.; Thiemann, T. Biosynthesis and metabolism of cyclopropane rings in natural compounds. *Chem. Rev.* **2003**, *103*, 1625−1648.
(39) Jamieson, C.; Moir, E. M.; Rankovic, Z.; Wishart, G. Medicinal Chemistry of hERG Optimizations: Highlights and Hang-Ups. *J. Med. Chem.* **2006**, *49*, 5029−5046.
(40) Romero, L.; Zamanillo, D.; Nadal, X.; Sánchez-Arroyos, R.; Rivera-Arconada, I.; Dordal, A.; Montero, A.; Muro, A.; Bura, A.; Segalés, C.; Laloya, M.; Hernández, E.; Portillo-Salido, E.; Escriche, M.; Codony, X.; Encina, G.; Burgueño, J.; Merlos, M.; Baeyens, J.; Giraldo, J.; López-García, J.; Maldonado, R.; Plata-Salamán, C.; Vela, J. Pharmacological properties of S1RA, a new sigma-1 receptor antagonist that inhibits neuropathic pain and activity-induced spinal sensitization. *Br. J. Pharmacol.* **2012**, *166*, 2289−2306.
(41) Cobos, E. J.; Baeyens, J. M.; Del Pozo, E. Phenytoin differentially modulates the affinity of agonist and antagonist ligands for ?1 receptors of guinea pig brain. *Synapse* **2005**, *55*, 192−195.
(42) Putman, K. P.; Bombick, D. W.; Doolittle, D. J. Evaluation of eight in vitro assays for assessing the cytotoxicity of cigarette smoke condensate. *Toxicol. In Vitro* **2002**, *16*, 599−607.
(43) (a) Maron, D. M.; Ames, B. N. Revised methods for the Salmonella mutagenicity test. *Mutat. Res.* **1983**, *113*, 173−215. (b) Reifferscheid, G.; Heil, J. Validation of the SOS/umu test using test results of 486 chemicals and comparison with the Ames test and carcinogenicity data. *Mutat. Res.* **1996**, *369*, 129−145.
(44) Amidon, G. L.; Lennernäs, H.; Shah, V. P.; Crison, J. R. A theoretical basis for a biopharmaceutic drug classification: the correlation of in vitro drug product dissolution and in vivo bioavailability. *Pharm. Res.* **1995**, *12*, 413−420.
(45) Wager, T. T.; Hou, X.; Verhoest, P. R.; Villalobos, A. Moving beyond rules: The development of a central nervous system multiparameter optimization (CNS MPO) approach to enable alignment of druglike properties. *ACS Chem. Neurosci.* **2010**, *1*, 435−449.
(46) Baell, J. B.; Holloway, G. A. New Substructure Filters for Removal of Pan Assay Interference Compounds (PAINS) from Screening Libraries and for Their Exclusion in Bioassays. *J. Med. Chem.* **2010**, *53*, 2719−2740.
(47) Box, K. J.; Comer, J. E. A. Using measured pKa, logP and solubility to investigate supersaturation and predict BCS class. *Curr. Drug Metab.* **2008**, *9*, 869−878.
(48) Chen, C.; Tran, J. A.; Tucci, F. C.; Chen, W. C.; Jiang, W.; Marinkovic, D.; Arellano, M.; White, N. Ligands of Melanocortin Receptors and Compositions and Methods Related Thereof. WO 2005040109, 2005.

https://doi.org/10.1021/acs.jmedchem.1c00417
J. Med. Chem. 2021, 64, 10139−10154